Tikrit Journal of Engineering Sciences (2025); 32(3): 2178
DOI: http://doi.org/10.25130/tjes.32.3.20

IRAQI Academic Scientific Journals

ISSN: 1813-162X (Print); 2312-7589 (Online)
Tikrit Journal of Engineering Sciences
available online at: http://www.tj-es.com

TJES Tikrit Journal of Engineering Sciences

Morphological, Physical, and Thermal Properties of Fly Ash Reinforced Low- and High-Density Polyethylene Composites: A Comprehensive Review

Saif S. Irhayyim *[a], Farouk M. Mahdi [a], Saad R. Ahmed [a], Sanjeev Khanna [b]
a Mechanical Department, College of Engineering, Tikrit University, Tikrit, Iraq.
b Department of Mechanical and Aerospace Engineering, University of Missouri Columbia, USA.

Keywords:
Polymer matrix composites; Fly ash; Physical properties; Thermal properties; HDPE; LDPE.

Highlights:

- Improved environmental sustainability by using fly ash waste in composites.
- Fly ash reduces the overall cost of polyethylene composites.
- Morphological analysis reveals a uniform dispersion of fly ash within the polymer matrix.
- Improved thermal stability observed in fly ash-reinforced polyethylene composites.
- Fly ash enhances the physical properties of LDPE and HDPE composites.

ARTICLE INFO
Article history:

Received	08 May 2024
Received in revised form	11 June 2024
Accepted	25 July 2024
Final Proofreading	03 July 2025
Available online	27 Aug. 2025

Citation: Irhayyim SS, Mahdi FM, Ahmed SR, Khanna S. **Morphological, Physical, and Thermal Properties of Fly Ash Reinforced Low- and High-Density Polyethylene Composites: A Comprehensive Review**. *Tikrit Journal of Engineering Sciences* 2025; **32**(3): 2178.
http://doi.org/10.25130/tjes.32.3.20

*Corresponding author:
Saif S. Irhayyim
Mechanical Department, College of Engineering, Tikrit University, Tikrit, Iraq.

Abstract: Due to their improved physical, rheological, and morphological properties, polyethylene/fly ash composites have been receiving considerable attention in recent years. This review comprehensively examines the properties of low- and high-density polyethylene/fly ash composites. Its structure is expounded in terms of how the polymer matrix interacts with FA particles. The review evaluates physical properties, including density, water absorption, and thermal stability, and examines the changes in these properties caused by FA reinforcement. The rheological properties of the produced composites, such as viscosity and elasticity, have also been reviewed to show how FA particles modify the processability and melt flow behavior of polyethylene matrices. This work also includes an in-depth examination of various techniques used in creating these composites, with an emphasis on the importance of selecting appropriate processing parameters to achieve optimal results. It also covers some important factors that may affect the performance of composites, including particle size, loading amount, and surface modification of FA particles. This review outlines the challenges and, hence, future research topics related to these issues. In this regard, it highlights the need for thorough research to optimize processing parameters, interface modification techniques, and advanced characterization methods. Generally, this review serves as a resourceful platform for researchers and engineers focused on enhancing the properties of advanced polymeric composites, targeting a broad spectrum of applications.

الخصائص المورفولوجية والفيزيائية والحرارية لمتراكبات البولي إيثيلين المنخفضة والعالية الكثافة المقواة بالرماد المتطاير: مراجعة شاملة

سيف صباح ارحيم[1]، فاروق منصور مهدي[1]، سعد رمضان احمد[1]، سانجيف خانا[2]

[1] قسم الهندسة الميكانيكية/ كلية هندسة / جامعة تكريت / تكريت - العراق.

[2] قسم الهندسة الميكانيكية / كلية هندسة / جامعة ميزوري كولومبيا/ الولايات المتحدة الامريكية.

الخلاصة

لقد جذبت متراكبات البولي إيثيلين - الرماد المتطاير اهتمامًا كبيرًا بسبب خصائصها الفيزيائية والريولوجية والمورفولوجية المحسنة. تبحث هذه المراجعة بدقة هذه الخصائص المتعلقة بمتراكبات البولي إيثيلين منخفض وعالي الكثافة - الرماد المتطاير. تتعمق المراجعة في الجوانب الهيكلية للمتراكبات، مع التركيز بشكل خاص على التشتت والالتصاق بين مصفوفة البوليمر وجسيمات الرماد المتطاير. تقوم المراجعة الحالية بتقييم الخصائص الفيزيائية بشكل شامل مثل الكثافة، وامتصاص الماء، والاستقرار الحراري وكيف يؤثر تعزيز الرماد المتطاير على هذه الخصائص. بالإضافة إلى ذلك، تحلل هذه المراجعة الخصائص الريولوجية للمواد المتراكبة، مثل اللزوجة والمرونة، لفهم كيفية تأثير جسيمات الرماد المتطاير على قابلية المعالجة وسلوك تدفق ذوبان مصفوفات البولي إيثيلين. علاوة على ذلك، توفر هذه المراجعة تحليلاً متعمقًا للطرق المختلفة المستخدمة لإعداد هذه المتراكبات، مع التأكيد على أهمية استخدام ظروف المعالجة المناسبة لتحقيق أفضل النتائج الممكنة. ويركز أيضًا على العوامل التي تؤثر على أداء المواد المتراكبة، مثل حجم الجسيمات، وكمية التحميل، وتعديل سطح جسيمات الرماد المتطاير. تسلط المراجعة الضوء على العقبات والمجالات المحتملة للبحث المستقبلي. ويؤكد على أهمية إجراء مزيد من التحقيقات لتحسين معلمات المعالجة، واستخدام تقنيات التعديل البينية، وتطوير أساليب التوصيف المتقدمة. بشكل عام، توفر هذه المراجعة موردًا قيمًا للباحثين والمهندسين الذين يعملون على متراكبات البوليمر المتقدمة لتعزيز خصائصها لمختلف التطبيقات.

الكلمات الدالة: الرماد المتطاير، متراكبات ذات الاساس البوليمري، النفايات البلاستيكية، الخصائص الحرارية، الخصائص الفيزيائية.

1.INTRODUCTION

Contemporary engineering applications require using unique materials with modern and distinct characteristics. Composite materials are a class of materials that harness the strengths of monolithic materials while mitigating their limitations. Optimization techniques can help mitigate the constraints of selecting and producing traditional materials. Moreover, properties can be tailored to meet specific design requirements and enable the fabrication of intricate geometries [1–3]. Composite materials have gained significant attention as engineering materials in recent years owing to their distinctive properties. This heightened interest is reflected in adopting design specifications that prioritize lightweight materials and high resistance. These materials have demonstrated efficacy in various domains, such as aerospace, transportation, civil engineering, and the medical sector. Composite materials are classified as materials that comprise a blend of constituent materials, which collectively provide the desired properties of the material. It is important to note that there is no chemical reaction between the constituent materials, and each component retains its intrinsic properties [4–6]. In today's fast-paced world, engineers and scientists eagerly anticipate the arrival of revolutionary materials distinguished by their low weight without sacrificing strength [3, 7]. Polymer Matrix Composites (PMCs) are widely used in everyday engineering applications due to their high strength-to-weight ratio. PMCs are comprised of a pliable polymeric matrix that is strengthened through reinforcements in the form of fibers, particles, or derived from waste biomass [1, 8, 9]. The interaction between the matrix and the reinforcement determines the mechanical performance of these composites. Although the stiffness of the composite is primarily influenced by the reinforcing component, including the percentage of reinforcement, its size, shape, structure, physical location, and orientation, the tensile strength is a combination of both the matrix and the reinforcement. Notably, the fabrication method is also critical in the composite's final properties [1, 10–12]. PMCs can potentially decrease the overall weight of structures, resulting in better fuel efficiency and enhanced performance in transportation applications. Thermoplastic matrix composites have been employed in engineering and semi-structural applications. Besides being easily fabricated using various forming techniques, thermoplastic polymers are also recyclable. These characteristics make them attractive for both present and future applications [13–15]. The importance of recycling plastic materials has grown in recent years due to environmental and ecological concerns. Due to rising landfill prices, decreasing landfill space, and growing environmental concerns, finding alternative methods to dispose of solid waste is becoming increasingly critical. However, plastic has a far lower recycling rate than paper and yard waste [16–18]. The global management of plastic waste before recycling is depicted in Fig. 1 [19]. The absence of efficient plastic recycling equipment significantly contributes to the industry's poor recycling rate. Synthetic polymers have long lifetimes because they are virtually completely resistant to biodegradation, whereas natural polymers have short lives since they are biodegradable. For environmental, financial, and especially power efficiency considerations, mechanical plastic recycling is a viable solution. However, the benefits become evident if recycles can replace virgin materials with little or no characteristic loss [20–22]. Waste materials, such as paper,

plastic, glass, and metal, are being utilized as raw materials instead of being disposed of in landfills, reducing the amount of raw materials needed and the volume of waste sent to landfills. Most post-consumer plastic waste comprises polyolefins, such as Polyethylene (PE) and Polypropylene (PP), with smaller amounts of Polystyrene (PS), PolyVinyl Chloride (PVC), and Polyethylene Terephthalate (PET) [10, 23–25]. Thermoplastics, especially PEs (High-Density Polyethylene (HDPE), Low-Density Polyethylene (LDPE), and Linear Low-Density Polyethylene (LLDPE)) and PP, account for approximately 60–70% of polymer waste, with PS (about 10–15%), PVC (about 15%), and PET (about 5%) making up the remainder. PEs and PP comprise most of the polymer waste and pose a formidable environmental threat when disposed of in landfills due to their nonbiodegradability. Due to their lower melting point, simplicity of processing on conventional plastic processing equipment at low temperatures, and cost-effectiveness; these thermoplastics are preferred over many others for recycling [14, 26, 27]. Recycling plastic materials remains a challenging task, requiring extensive research by manufacturers and scientists. Nevertheless, recycling often results in the deterioration and loss of mechanical properties of the recycled material. Cross-linking, adding particulate or fibrous additives, and modifying the material can recover some of its properties and broaden its spectrum [28–30]. The adverse effects of plastic pollution on human well-being are extensive and multifaceted, affecting areas such as the aesthetic appeal of beaches, the functioning of drainage and wastewater systems, and serving as breeding sites for disease-spreading organisms. The sun's ultraviolet light causes the plastic to break down into small fragments, known as "microplastics," which are challenging to remove, disrupt the food chain, and harm natural habitats [31–34]. The main issues associated with post-consumer recycling are degradation during the product's lifetime and contamination of the material with other substances, which decreases the quality of the recycled materials, making them unsuitable for use in specific applications. Various methods have been developed to improve the quality of recycled materials, such as mechanical and chemical treatments [10,34,35].

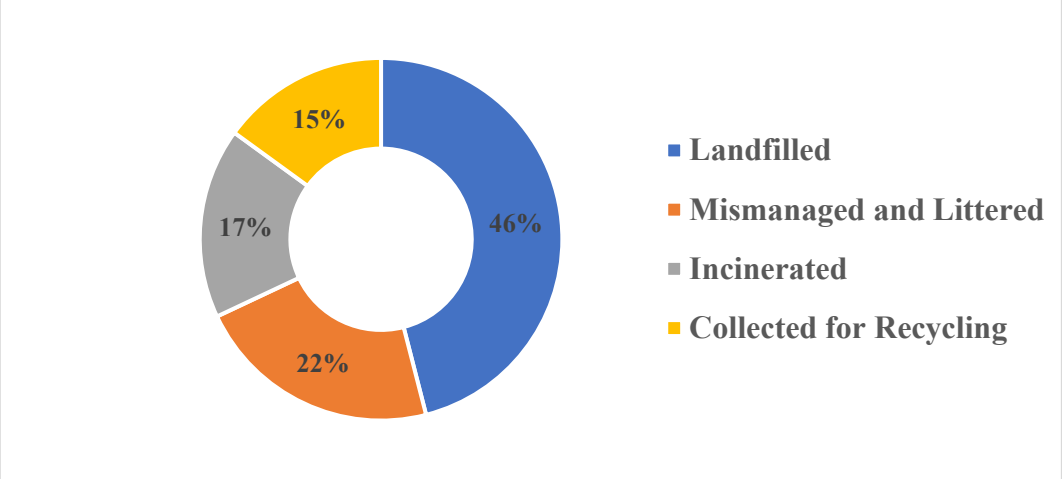

Fig. 1 The Global Management of Plastic Waste before Recycling [19].

PE is an integral component in various industries, particularly packaging, and is extensively used in manufacturing a diverse range of commercial products. Figure 2 depicts how plastics are distributed globally across different sectors due to their comparatively low cost, resistance to moisture and other oxidizing agents, and adequate capacity to elongate and withstand surface impacts [19, 36, 37]. Additionally, PE is recognized as an effective polymer for preventing erosion. Generally, various filler forms are introduced into polymer matrices to regulate their mechanical, thermal, and rheological properties. Numerous investigations have explored PE's thermal and mechanical properties combined with inorganic metallic fillers. It is well-known that the properties of particulate-filled polymer composites are influenced by the size, shape, and distribution of filler particles within the polymeric matrix, as well as their adhesion at the interface [38, 39]. Studies on applying Fly Ash (FA) as a filler in polymer matrices have mainly focused on their mechanical, morphological, and dielectric properties. Incorporating FA in PE significantly enhances its compression properties, thus rendering FA thermoplastic composites a feasible alternative for structural applications. The incorporation of FA in both virgin and recycled thermoplastic matrices, such as PP, HDPE, and LDPE, has also demonstrated encouraging outcomes regarding their tensile properties [40–42].

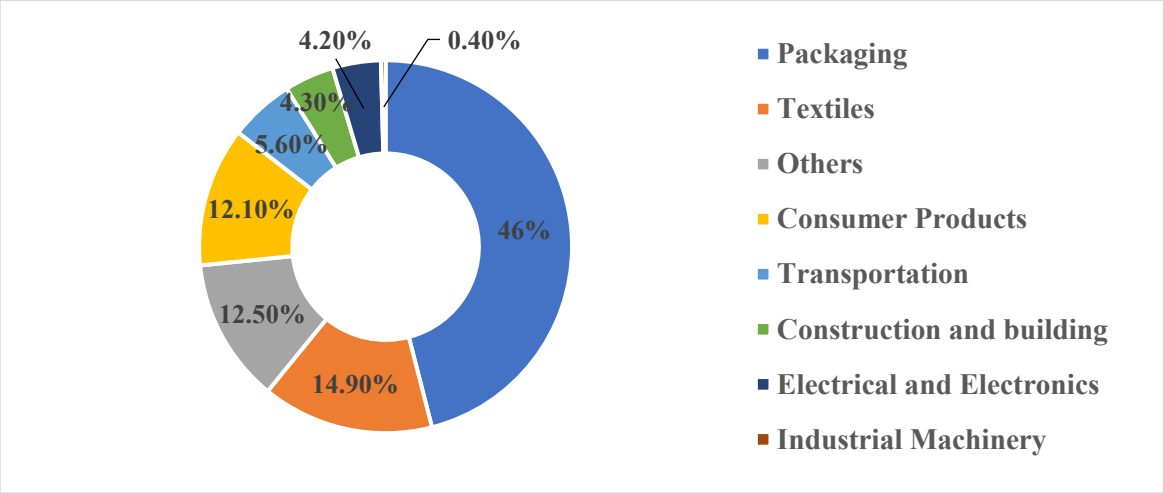

Fig. 2 Worldwide Distribution of Plastics in Many Industries [19].

FA can originate from various sources, such as municipal solid waste, biomass, oil, and coal. Over a brief timeframe, the exponential rise in population significantly increases municipal solid waste generation. Conventional primary waste management techniques, such as disposal in landfills, have proven inadequate in handling the sheer volume of household solid waste produced [43–45]. As a result, incineration of municipal solid waste has been a long-standing practice. However, using incineration as a waste management approach or as an energy source is limited by generating FA and bottom ash [45–47]. FA is a byproduct material generated from burning coal and fuel in power plants collected during combustion. It is categorized into two primary forms: Coal Fly Ash (CFA) and Oil Fly Ash (OFA), depending on the type of energy utilized during combustion. FA is a fine-ground particulate material. The composition of OFA primarily consists of carbon black, unburned carbon, and a limited quantity of sulfur and oxides, which may vary based on the fuel utilized [48–51]. Coal-fired power plants produce four primary byproducts from coal combustion: CFA, bottom ash, boiler ash, and flue gas desulphurization gypsum. Coal combustion products comprise approximately 40% of CFA waste. CFA is a residual material collected from flue gases through electrostatic precipitators or filter fabric collectors. Figure 3 shows that the CFA is composed mainly of Si_2O_3 and Al_2O_3, along with CaO, Fe_2O_3, MgO, and SO_3 [45, 52, 53].

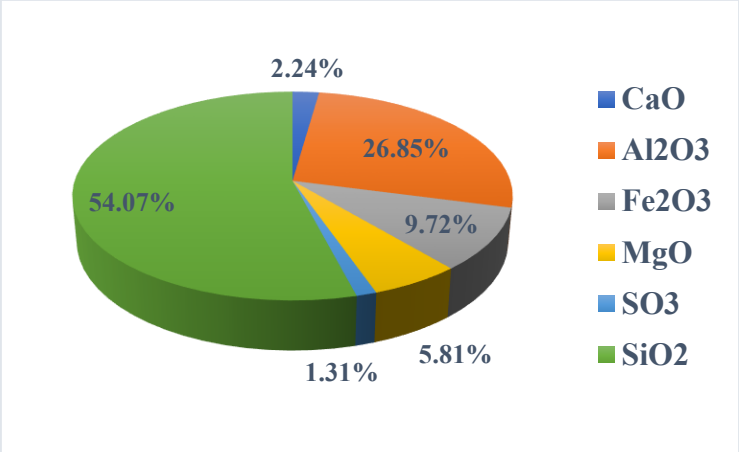

Fig. 3 The Main Chemical Composition of CFA [53].

Cenosphere Coal Fly Ash (CCFA) are inert hollow silicate spheres. These naturally occurring byproducts are generated during coal burning in power plants and exhibit similar properties to commercially manufactured hollow-sphere products. CCFAs have found widespread use in various applications, such as plastics, rubbers, resins, and types of cement, where they serve as fillers or lubricants [41, 54, 55]. CCFAs were first introduced in the United States as plastic compounds' extenders due to their compatibility with plastisol's thermoplastics, Latex, Polyesters, Epoxies, Phenolic resins, and urethanes. Their compatibility with specialized cement, adhesives, coatings, and composites has also been extensively explored. CCFAs have many applications, including sports equipment, insulation, automobile bodies, marine craft bodies, paints, and fire and heat protection devices. They are typically employed in gypsum board jointing compounds, veneering plasters,

stuccos, sealants, coatings, and cast resins. The advantages of CCFAs in these applications include reduced weight, increased filler loadings, better flow characteristics, less shrinkage and warping, and reduced water absorption [13, 54, 56]. The present work details a comprehensive review of the physical, morphological, and rheological characteristics of LDPE and HDPE composites reinforced with FA particles. By synthesizing the information from these characterization techniques, this review aims to provide a better understanding of how the FA complexly influences the structure-property relationships of such composites at nano- to macroscales. This work, therefore, provides insight into how these wonder particles could be utilized to enhance composite performance. This work has, therefore, contributed to a better understanding of the exciting potential for improvements through detailed investigations into the dispersion/distribution of FA particles, interfacial interactions, and the resulting microstructure. More importantly, the positive influence that FA incorporation brought about was investigated through the measurement of physical properties relevant to density, water absorption, aging behavior, and thermal stability. The rheological behavior of composites can also be used to understand the processing and flow behavior of such materials. In this way, it becomes possible to determine the optimal conditions for processing. Hence, the main objective of this research is to study how the FA properties, in terms of size, shape, and chemical composition, impact the characteristics and behaviors of polyethylene, as well as the interactions of the latter with the matrix and the particles of reinforcement. These interactions can then impact spherulitic crystallization, thermal stability, melt rheology, and tensile behavior, exposing significant structure-property linkages that have remained relatively unexplored. With an improved understanding, one can develop more effective composite formulations for various industrial applications. The present review summarizes existing knowledge, presents a novel perspective on LDPE and HDPE composites with FA particles, and suggests future research directions in both academic circles and industrial applications.

2.MATERIALS USED FOR FABRICATING POLYETHYLENE COMPOSITES

The production of thermoplastic polymer composites involves combining the polymer and reinforcement, which are poured into pre-made molds. Numerous patents showed that researchers and industrialists have successfully employed the traditional blending method [57, 58]. Blending technology has advanced significantly, from non-intermeshing to continuous mixtures and from single-screw extrusion to co-rotating twin-screw extrusion. A two-step process is required to create PE and FA composites. Firstly, the matrix and reinforcement are mixed to form a uniform and consistent structure. After that, the mixture is shaped into the desired form using an injection molding machine [1, 59, 60]. Table 1 summarizes various research studies on fabricating PE matrix composites reinforced with FA particles and their hybrid composites. The table includes two types of PE matrices: HDPE and LDPE, which are obtained from both virgin and recycled sources. The studies incorporated different types of FA particles, including OFA, CFA, and CCFA, with varying particle sizes on both the microscale and nanoscale. Among these, CFA was the most frequently used reinforcement material, primarily due to its ability to enhance the mechanical properties of PE matrix composites. Furthermore, CFA is also one of the world's largest industrial waste-to-power plants. Researchers studied the impact of FA on the PE matrix composite. Weight percentages, particle size, and silane treatment were the most influential factors in the properties of the composite. The effect of FA type and characteristics on the mechanical properties, thermal stability, and morphological characteristics of FA-reinforced PE composites has been extensively studied. Mechanical properties, such as tensile strength, flexural strength, impact resistance, and hardness, were studied the most. Besides, tribological characteristics have not been extensively studied in previous research. However, the study of composites made of PE reinforced with FA has provided useful insights into optimizing the material's performance for various applications. These applications include the construction and automotive industries, packaging, and electrical components.

Table 1 Selective Studies Focus on Fabricating HDPE and LDPE Matrix Composites Reinforced with FA Particles and Their Hybrid Composites.

1- High-density Polyethylene (HDPE) Matrix Composites:

No.	Matrix + Reinforcement	Fabrication Method	Studied Variables	Studied Properties	Ref.
1.	- RHDPE + Calcium Carbonate (CC). - RHDPE + untreated CFA. - RHDPE + treated CFA.	Mixing is performed using a Thermo Haake Rheomixer, followed by compression molding in a Carver polymer press.	- RHDPE + 0, 10, 20, 30, 40 wt.% CC. - RHDPE + 0, 10, 20, 30, 40 wt.% untreated CFA. - RHDPE + 0, 10, 20, 30, 40 wt.% treated CFA.	- Tensile properties according to ASTM D 638 (Type IV). - Morphological properties of the fracture surface of tensile specimens.	[10]
2.	HDPE (grade: 24FS040) + silane-treated CCFA + HDPE-g-DBM.	Mixing by Brabender melt mixer followed by injection molding.	HDPE + 0, 10, 20, 30 vol. % CCFA (silane treated) + 0, 5, 10, 15 % HDPE-g-DBM.	- Tensile properties according to ASTM D 1708. - Thermal properties. - Morphological properties of the fracture surface of tensile specimens.	[54]
3.	HDPE (grade: M60075) + CFA.	Mixing is performed using a co-rotating twin-screw extruder followed by injection molding.	HDPE + 0, 5, 10, 15, 20, 30, 40 wt.% CFA + (14 µm), (22 µm), and (50 µm) particle size of CFA.	- Tensile properties according to ASTM D 638. - Flexural properties according to ASTM D 790. - Izod impact properties according to ASTM D256. - Morphological properties of the fracture surface of tensile specimens.	[61]
4.	- HDPE (grade: HD53EA 010) + CCFA. - HDPE (grade: HD53EA 010) + silane-treated CCFA.	Mechanical mixing by two roll mills followed by compression molding.	- HDPE + 0, 10, 15, 20 wt. % CCFA. - HDPE + 0, 10, 15, 20 wt. % silane-treated CCFA. - Abrasive wear measurements at 10 N applied load on the sliding distance at 9.42, 18.84, 28.26, and 37.68 m for 100 rpm (0.314 m/s), 200 rpm (0.628 m/s) and 300 rpm (0.942 m/s).	- Tensile properties according to ASTM D 638. - Izod impact properties according to ASTM D256. - Shore D hardness according to ASTM D 2240. - Abrasive wear measurements on a single pin-on-disc machine. - Densities measurement according to Archimedes' principle. - Morphological properties and XRD of the surface of the abrasive wear specimens.	[56]
5.	HDPE + CFA.	Mechanical mixing with xylene medium followed by compression molding.	HDPE + 0, 3, 5, 10, 15, 20, 30, 40, 50, 70 vol.% CFA.	- Thermal properties.	[40]
6.	- Waste Polyethylene (WPE) (HDPE + LDPE + LLDPE + PP + PS) + CFA. - WPE (HDPE + LDPE + LLDPE + PP + PS) + Coal Nano Fly Ash (CNFA). - MA-g-WPE + CFA. - Irradiated WPE + CFA. - WPE + irradiated CFA. - MA-g-WPE + CNFA - Irradiated WPE + CNFA - WPE + irradiated CNFA.	Mixing by Brabender melt mixer followed by compression molded between Teflon sheets.	- WPE + 0, 5, 10, 20 wt. % CFA. - WPE + 0, 1, 3, 5, 7 wt. % CNFA. - MA-g-WPE + 5 wt. % CFA. - Irradiated WPE + 5 wt. % CFA. - WPE + 5 wt. % irradiated CFA. - MA-g-WPE + 5 wt. % CNFA. - Irradiated WPE + 5 wt. % CNFA. - WPE + 5 wt. % irradiated CNFA.	- Tensile properties according to ASTM D 638 (Type IV). - Flexural properties according to ASTM D 790. - The tensile impact energy according to DIN 53448. - Shore D hardness according to ASTM D 1132. - Thermal properties. - Dynamic Mechanical Analysis. - Electron Beam Irradiation Analysis. - Morphological properties of the fracture surface of tensile specimens. - Aging Studies according to ASTM D 573.	[62]
7.	- HDPE (grade: B 6401) + CFA. - HDPE (grade: B 6401) + CNFA. - MA-g-HDPE + CFA - Irradiated HDPE + CFA - HDPE + irradiated CFA. - MA-g-HDPE + CNFA - Irradiated HDPE + CNFA - HDPE + irradiated CNFA.	Mixing by Brabender melt mixer followed by compression molded.	- HDPE + 0, 5, 10, 20 wt. % CFA. - HDPE + 0, 1, 3, 5, 7 wt. % CNFA. - MA-g- HDPE + 5 wt. % CFA. - Irradiated HDPE + 5 wt. % CFA. - HDPE + 5 wt. % irradiated CFA. - MA-g- HDPE + 5 wt. % CNFA. - Irradiated HDPE + 5 wt. % CNFA. - HDPE + 5 wt. % irradiated CNFA.	- Tensile properties according to ASTM D 638 (Type IV). - Flexural properties according to ASTM D 790. - The tensile impact energy according to DIN 53448. - Shore D hardness according to ASTM D 2240. - Thermal properties. - Dynamic Mechanical Analysis. - Electron Beam Irradiation Analysis. - Morphological properties of the fracture surface of tensile specimens. - Aging Studies according to ASTM D 573.	[38]
8.	- (WPE/HDPE: 50/50 blend (WH)) + CFA. - (WPE/HDPE: 50/50 blend (WH)) + CNFA. - MAWH + CFA. - Irradiated WH + CFA. - WH + irradiated CFA. - MAWH + CNFA. - Irradiated WH + CNFA. - WH + irradiated CNFA.	Mixing by Brabender melt mixer followed by compression molded.	- WH + 0, 5, 10, 20 wt. % CFA. - WH + 0, 1, 3, 5, 7 wt. % CNFA. - MAWH + 5 wt. % CFA. - Irradiated WH + 5 wt. % CFA. - WH + 5 wt. % irradiated CFA. - MAWH + 5 wt. % CNFA. - Irradiated WH + 5 wt. % CNFA. - WH + 5 wt. % irradiated CNFA.	- Tensile properties according to ASTM D 638 (Type IV). - Flexural properties according to ASTM D 790. - The tensile impact energy according to DIN 53448. - Shore D hardness according to ASTM D 2240. - Thermal properties. - Dynamic Mechanical Analysis. - Electron Beam Irradiation Analysis. - Aging Studies according to ASTM D 573.	[63]
9.	- RHDPE + Coir Fiber (CF). - RHDPE + CF + MA-g-HDPE. - RHDPE + CF + MA-g-HDPE + CCFA.	Mixing is achieved by intermeshing counter-rotating JSW twin-screw extruder, followed by injection molding.	- RHDPE + 0, 10, 20, 30, 40 wt.% CF. - RHDPE + 30 wt.% CF + 1, 3, 5 wt.% MA-g-HDPE. - RHDPE + 30 wt.% CF + 1 wt.% MA-g-HDPE + 2.5, 5, 7.5, 10 wt.% CCFA.	- Tensile properties according to ASTM D 638. - Flexural properties according to ASTM D 790. - Izod impact properties according to ASTM D256. - Shore D hardness according to ASTM D 2240. - Water Absorption Measurement according to ASTM D570. - Thermal properties. - Morphological properties of the fracture surface of tensile specimens. - Dynamic Mechanical Analysis.	[28]

10.	- HDPE (grade: HD50MA180) + CCFA. - HDPE (grade: HD50MA180) + silane-treated CCFA.	Mechanical mixing followed by injection by a single screw extruder machine	- HDPE + 0, 20, 40, 60 wt. % CCFA. - HDPE + 0, 20, 40, 60 wt. % silane-treated CCFA.	- Tensile properties according to ASTM D 638. - Densities measurement according to ASTM D 792. - Morphological properties.	[13]
11.	- HDPE + Ultra Fine Fly Ash (UFFA) + Multi-Walled Carbon Nano Tubes (MWCNT).	Mixing by Brabender melt mixer followed by compression molded	HDPE + 20, 19.8, 19.6, 19.2, 18.5 wt.% UFFA + 0, 0.2, 0.4, 0.8, 1.5 wt.% MWCNT.	- Tensile properties according to ASTM D638. - Flexural properties according to ASTM D790. - Thermal properties. - FTIR Spectroscopy. - Morphological properties and XRD.	[64]
12.	RHDPE + CFA	Mechanical rotational mixing by a PE mill followed by injection molding.	RHDPE + 0, 2.5, 5, 7.5, 10 wt.% CFA	- Tensile properties according to ASTM D638. - Charpy impact strength according to ASTM D6110. - Morphological properties of the fracture surfaces.	[65]
13.	- RHDPE + Banana Fiber (BF). - RHDPE + BF + MA-g-HDPE. - RHDPE + BF + MA-g-HDPE + CCFA.	Mixing is achieved by intermeshing the counter-rotating the JSW twin-screw extruder, followed by injection molding.	- RHDPE + 0, 10, 20, 30 wt.% BF. - RHDPE + 30 wt.% BF + 1, 3, 5 wt.% MA-g-HDPE. - RHDPE + 30 wt.% BF + 3 wt.% MA-g-HDPE + 2.5, 5, 7.5, 10 wt.% CCFA.	- Tensile properties according to ASTM D638. - Flexural properties according to ASTM D790. - Izod impact properties according to ASTM D256. - Shore D hardness according to ASTM D2240. - Water Absorption Measurement according to ASTM D570. - Thermal properties. - Morphological properties of the fracture surface of tensile specimens. - Dynamic Mechanical Analysis.	[41]
14.	HDPE (grade: HD50MA180) + CFA.	Manually mixed in solvent (acetone) and then mechanically mixed by counter-rotating twin-screw extruder followed by injection molding.	HDPE + 0, 5, 10, 15, 20, 25 wt.% CFA	- Tensile properties according to ASTM D 638. - Flexural properties according to ASTM D 790. - Thermal properties. - Rheological properties. - Morphological properties. - Dynamic Mechanical Analysis.	[42]
15.	- RHDPE + Jute Fiber (JF). - RHDPE + JF + MA-g-HDPE. - RHDPE + JF + MA-g-HDPE + CCFA.	Mixing is achieved by intermeshing the counter-rotating the JSW twin-screw extruder, followed by injection molding.	- RHDPE + 0, 10, 20, 30 wt.% JF. - RHDPE + 20 wt.% JF + 1, 3, 5 wt.% MA-g-HDPE. - RHDPE + 20 wt.% JF + 3 wt.% MA-g-HDPE + 2.5, 5, 7.5, 10 wt.% CCFA.	- Tensile properties according to ASTM D 638. - Flexural properties according to ASTM D 790. - Izod impact properties according to ASTM D256. - Shore D hardness according to ASTM D2240. - Water Absorption Measurement according to ASTM D570. - Thermal properties. - Morphological properties of the fracture surface of tensile specimens. - Dynamic Mechanical Analysis.	[66]
16.	HDPE (grade: HD50MA180) + CCFA.	Mixing by single screw extruder followed by 3D printing.	- HDPE + 0, 20, 40, 60 vol.% CCFA. - Compressive behavior under quasi-static strain rates (0.001, 0.01, 0.1 s^{-1}).	- Quasi-static compression test. - Morphological properties.	[67]
17.	HDPE (grade: SABIC P6006N) + OFA.	Mixing using a HAAKE PolyLab melt mixer, followed by injection molding.	- HDPE + 10 wt.% (OFA1(50–90 µm), OFA2 (90–150 µm), and OFA3 (150–250 µm)). - The fresh samples were recycled four times by using an extrusion plastometer.	- Tensile properties according to ASTM D 638. - Thermal properties. - Morphological properties.	[68]
18.	- HDPE (grade: DGDA-2502NT) + silane-treated CFA masterbatch. - HDPE (grade: DGDA-2502NT) + silane treated CFA masterbatch + HDPE-g-MAH.	- Mixing by a micro compounder extruder followed by injection molding. - FEA.	- HDPE + 0, 5, 10, 15, 20 % wt. silane treated CFA. - HDPE + 10 % wt. silane treated CFA + 5, 10, 15 wt.% HDPE-g-MAH.	- Tensile properties according to GB/T 1040.2-2006. - Thermal properties. - FTIR Spectroscopy. - Morphological properties.	[69]
19.	HDPE (grade: SABIC P6006N) + OFA.	Mixing is done using a HAAKE PolyLab melt mixer, followed by injection molding.	- HDPE + 5, 10, 15 wt.% OFA. - Aging Tests for 0, 5, 10, 15, and 20 weeks at cycles being: (1) UV-A: 1.55 W/m2/nm, 60 C, 8 h. (2) Condensation: 50 C, 4 h.	- Tensile properties according to ASTM D 638. - Thermal properties. - Morphological properties. - Aging Studies.	[70]
20.	RHDPE + Rice Husk Ash (RHA) + CFA	Mixing by 3D Rotary mixer followed by hot pressing.	- RHDPE. - RHDPE + 5 wt.% RHA + 5 wt.% CFA. - RHDPE + 10 wt.% RHA + 10 wt.% CFA. - RHDPE + 15 wt.% RHA + 15 wt.% CFA.	- Tensile properties according to ASTM D 1822L. - Shore D hardness according to ASTM D 2240. - Morphological properties.	[71]

2- Low-Density Polyethylene (LDPE) Matrix Composites:

No.	Matrix + Reinforcement	Fabrication Method	Studied Variables	Studied Properties	Ref.
1.	- LDPE + OFA - LDPE + OFA + PE-g-MA. - LDPE + COOH-OFA - LDPE + COOH-OFA + PE-g-MA.	Mixing was performed using a Brabender melt mixer, followed by compression molding in a Carver polymer press.	- LDPE + 0, 1, 2, 5, 10 wt.% OFA. - LDPE + 0, 1, 2, 5, 10 wt.% OFA + 2 wt.% PE-g-MA. - LDPE + 0, 1, 2, 5, 10 wt.% COOH-OFA. - LDPE + 0, 1, 2, 5, 10 wt.% COOH-OFA + 2 wt.% PE-g-MA.	- Morphological properties. - Rheological properties.	[72]
2.	- LDPE + OFA - LDPE + OFA + PE-g-MA. - LDPE + COOH-OFA - LDPE + COOH-OFA + PE-g-MA.	Mixing was performed using a Brabender melt mixer, followed by compression molding in a Carver polymer press.	- LDPE + 0, 1, 2, 5, 10 wt.% OFA. - LDPE + 0, 1, 2, 5, 10 wt.% OFA + 2 wt.% PE-g-MA. - LDPE + 0, 1, 2, 5, 10 wt.% COOH-OFA. - LDPE + 0, 1, 2, 5, 10 wt.% COOH-OFA + 2 wt.% PE-g-MA.	- Tensile properties according to ASTM D 638. - Thermal properties. - Morphological properties.	[48]
3.	- LDPE (grade: 16MA400) + CCFA. - LDPE (grade: 16MA400) + silane-treated CCFA.	Mechanical mixing by two roll mills, followed by compression molding.	- LDPE + 0, 10, 15, 20 wt. % CCFA. - LDPE + 0, 10, 15, 20 wt. % silane-treated CCFA. - Abrasive wear measurements at 10 N applied load on the sliding distance at 9.42, 18.84, 28.26, and 37.68 m for 100 rpm (0.314 m/s), 200 rpm (0.628 m/s) and 300 rpm (0.942 m/s).	- Tensile properties according to ASTM D 638. - Izod impact properties according to ASTM D256. - Shore D hardness according to ASTM D 2240. - Abrasive wear measurements on a single pin-on-disc machine. - Density measurement is according to Archimedes' principle. - Morphological properties and XRD of the surface of the abrasive wear specimens.	[55]
4.	LDPE + CFA + CC	Mixing the mixture in an aluminum pot and casting into a metallic mold.	- 50 wt. % LDPE + 0/0, 10/40, 20/30, 30/20, 40/10, 45/5 wt.% CFA/CC. - Water Absorption at 24, 48, 72, 96, 120, 144, 168 hrs. soaking time.	- Density measurement. - Water Absorption measurement. - Rheological properties. - Flexural properties according to ASTM D7264. - Micro - HV. - Thermal properties. - FTIR Spectroscopy.	[73]
5.	LDPE + CFA	Mixing manually followed by injection molding in a single screw injection molding machine	LDPE + 0, 1, 5, 20, 50 wt.% CFA + (0-15 µm), (15-30 µm), (30-60 µm) CFA	- Tensile properties. - Compression properties. - HB test. - Thermal properties. - Flammability test. - Morphological properties.	[74]
6.	- LDPE + CFA. - LDPE + CFA + Triphenyl Phosphate (TPP).	Mixing by single screw extruder followed by compression molding.	- LDPE + 0, 5, 10, 15, 20 wt.% CFA. - LDPE + 20 wt.% CFA + 1, 2, 5 wt.% TPP.	- Tensile properties according to ASTM D638. - Thermal properties. - Density measurement. - Resistance to different chemical reagents according to ASTM D543-14. - Flammability test according to ASTM D635. - Water Absorption Measurement according to ASTM D570.	[75]

3.MORPHOLOGICAL ANALYSIS

3.1.Scanning Electron Microscopy (SEM)

Utilizing waste products, such as FA, as fillers in polymer composites has led to innovative ideas to improve their performance. Mixing and blending precalles directly impact whether the desired result can be achieved. To ensure everything is compounded effectively, obtaining a uniform and optimal dispersion of the particles is important, as this determines how well the filler interacts with the host polymer. The morphology of the polymer composites reinforced with FA was found to be influenced by many parameters, including (1) polymer type, (2) method of preparation, (3) FA types, content, particle size, and distribution, (4) surface modification, and (5) synergy with other fillers [45, 76, 77].

3.1.1.High-Density Polyethylene Matrix Composites

According to the investigation conducted by Atikler et al. [10], including CFA and CC fillers in Recycled High-Density Polyethylene (RHDPE) composites, the mechanical properties, such as tensile strength and Young's modulus, were enhanced. In particular, Field Emission Scanning Electron Microscopy (FESEM) studies provided irrefutable proof of superior interfacial adhesion between the CFA filler and the RHDPE matrix, demonstrating that the silane treatment resulted in higher mechanical properties, which suggests that using waste materials in novel areas makes creating new composite materials with improved mechanical properties and characteristics possible. Deepthi et al. [54] studied the morphological features of HDPE/CCFA composites with the addition of a compatibilizer. From SEM micrographs of etched surfaces, it was observed that the un-compatibilized blend containing 20% CCFA loading consisted of large holes created by the pullout of clustered CCFA particles. The presence of some elongated voids indicates a slight resistance to particle removal, suggesting that an interaction may exist between the filler and the matrix. It was due to the salinization treatment of CCFAs that would have reduced interfacial tension between the filler and the matrix. In contrast, improved interfacial adhesion and blend morphology were pointed out by the compatibilized blend, which exhibited a rough surface and elongated voids.

Ahmad et al. [61] reported that the particle size distribution of CFA was found to have a significant impact on the mechanical properties of HDPE composites. The SEM image revealed the formation of voids at the CFA–HDPE interfaces, which coalesced upon elongation and led to fracture or breakage. The void concentration increased with the CFA concentration, reducing elongation at break. The SEM image also showed that small CFA particles, less than three μm, insignificantly caused the fracture. The SEM image presented in Fig. 4 (a) provided insight into the failure mechanism under tensile stress, as illustrated schematically in Fig. 4 (b).

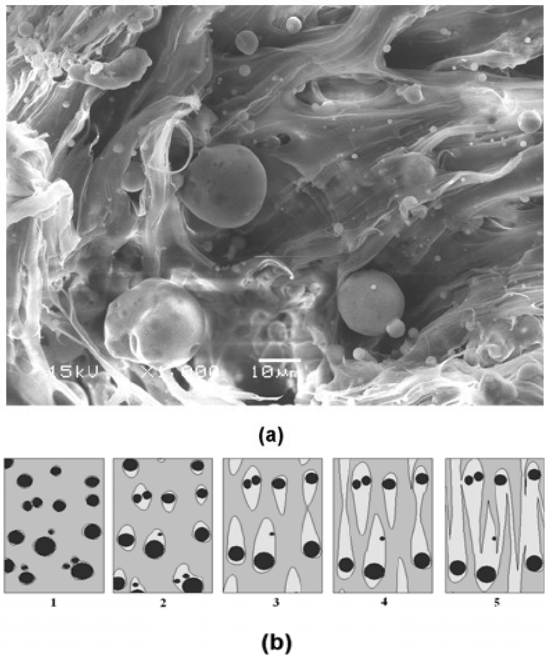

Fig. 4 (a) SEM Micrographs at 1000X Showing the Mechanism of Failure of Tensile Fractured Surface. (b) Schematic Illustration of Tensile Fracture in Steps [61].

Satapathy et al. [62] studied the morphological properties of CFA and CNFA-filled WPE composites. The fractured surfaces of the tensile specimens of the CFA/CNFA-filled WPE hybrid composites were examined under an SEM. The following observations were made. On the other hand, from the SEM images of the fractured surfaces of the composites, the CFA/CNFA particles appeared to behave like stress raisers, thus arresting crack propagation and improving the performance properties of the composites. Evidence of plastic deformation was shown on the fractured surface of WPE, as indicated by the broad flow lines. In contrast, the tensile-fractured surface of WPE + 5% CFA shows large voids along with irregular patterns. In the case of MA-g-WPE + 5% CFA, the surface appears to be well-knit, and the CFA particles seem to be well-embedded in the modified matrix. It has also been found that the CFA/CNFA particles are well dispersed in the WPE matrix, as indicated by the SEM images. It can be noted that SEM images of irradiated composites revealed a rough surface of the particles, indicating that electron-beam irradiation causes the surface modification of the particles, which enhances the properties of the composites. Satapathy et al. [38] studied the surface topography of the tensile fracture surfaces by SEM for HDPE-CFA/CNFA composites. In their work, SEM micrographs of the fractured surfaces of tensile tested HDPE-CNFA, MA-g-HDPE-CNFA, HDPE-CNFA (irr.), and HDPE-irr. CNFA composites were taken and discussed. Before examination, the fracture surfaces were sputter-coated with a thin layer of gold in a vacuum chamber. The SEM images of composites that incorporated CFA/CNFA into the HDPE matrix showed improved interfacial adhesion and better compatibility of the filler dispersion with the matrix. The modified composites depicted a more homogeneous distribution of particles of CFA/CNFA inside the HDPE matrix, along with better dispersion. It was further observed that the electron beam-irradiated HDPE-CFA/CNFA composite, as shown in the SEM micrograph, is more compact with fewer voids and a homogeneous structure compared to the pristine composites. The results from the SEM analysis also disclosed that the modification, mainly MA grafting, has altered the surface morphology and particle distribution. More importantly, MA grafting improved the interfacial adhesion between the matrix and filler particles by increasing the surface roughness. Satapathy et al. [63] further investigated the morphology of fractured samples of WH-CFA/CNFA after a tensile test using SEM. The fracture surfaces were sputter-coated with a thin layer of gold in the vacuum chamber before examination. SEM studies showed that the addition of CFA/CNFA to the WH blend matrix results in better dispersion of fillers within the matrix without the formation of visible agglomerates. Further modifications introduced into the WH/HDPE-CFA/CNFA composite improved the dispersion of fillers within the matrix. Electron beam irradiation of WH-CFA/CNFA composites showed the best distribution of fillers among all other modifications. These results demonstrate that the irradiated WH-CFA/CNFA composite can be used as an engineering material with homogeneous filler dispersion. Satapathy et al. [28] studied the morphological properties of the biocomposites using SEM. In the reported SEM images, most of the CCFA particles were found to be spherical, with smooth surfaces. From the SEM study, it was observed that the CCFA and RHDPE grids were well inter-linked, increasing the hardness and sensitivity of the biocomposites, thereby improving their flexural properties without much effort, even under severe conditions. The SEM study explained

that the addition of CF into the RHDPE matrix increased its modulus because the fibers brought about the strengthening effect that allows more stresses to be transferred at the contact, thus increasing its load-bearing capacity. Kumar et al. [13] utilized SEM for microstructural analysis of the syntactic foam composites filled with untreated and silane-treated CCFA. These SEM images showed that CCFA-filled cross-linked PE composites dispersed relatively homogeneously within the HDPE matrix, with a relatively strong interfacial adhesion between the two components. The results of the SEM test also proved that the specimens of the syntactic foam had a relatively smooth surface, indicating that the polymer injection molding process effectively produced high-quality samples. All the above-mentioned results prove that the composites have excellent mechanical properties. Khan et al. [64] reported on the SEM analysis of blends containing HDPE, MWCNT, and UFFA. From the SEM micrographs of the composite material subjected to compatibilization without the addition of MWCNT, it can be observed that the prevailing mode of failure is of a quasi-brittle nature, wherein the matrix deforms, and the surface texture is relatively rough. Moreover, the particles are dispersed uniformly and are embedded within the matrix-entangled network. The fracture mode of the 0.2% MWCNT-filled composite material with UFFA was found to be quasi-brittle, characterized by deformation and shear deformation of the matrix. Upon increasing magnification, as shown in the image below, areas of ductility with extended voids were created due to particle cavitation, besides debonded and trapped particles within the matrix. In the SEM images, it was observed that the agglomerated particles, consisting of UFFA and MWCNTs, were evenly distributed in the matrix for nanocomposites with 0.2% and 0.4% MWCNTs. Agglomerated particles of the stream in the matrix promoted stress transfer from the matrix to the filler, suggesting that interfacial bonding had improved. As observed in the SEM micrographs of FA, there was a tendency for the fine particles to agglomerate and form clusters. Kabir et al. [65] utilized the SEM to study the microstructure of composites fabricated from CFA and RHDPE. As shown in their research, the role of silane coupling agents and compatibilizers in debonding and cavitation avoidance was studied. This study primarily determined the transitions based on dependent variables, including dispersant volume, particle size, intrinsic flaw size, generated flaw size, and the strength of the dispersant-matrix bond, together with its associated effectiveness in load transfer. Principally, fibril failure, accompanied by restricted plastic deformation and genuine brittle failure behavior, characterized the microstructures of the composites. From the SEM images, a very smooth surface of pure RHDPE with negligible undulations was observed, indicating a fragile fracture. The incorporation of CFA resulted in a change to a coarse and uneven texture, suggesting a shift in behavior from brittle to ductile mode. It is observed that SEM images reveal the presence of voids on the fracture surfaces of specimens containing CFA, indicating poor interfacial adhesion between the CFA particles and the RHDPE matrix. The obtained SEM images conformed to the mechanical data and showed the trend for impact resistance and tensile strength. The SEM images reflected void formation, ligament formation, and crazing. These phenomena were attributed to the concentration of stresses, debonding, and cavitation. Satapathy et al. [41] studied the effect of BF and CCFA on the RHDPE composites using SEM. From the SEM micrographs, the uniform distribution of bast fibers in the RHDPE matrix and the complete embedding of the fibers into the matrix are revealed. This research demonstrated that the addition of CCFA to the RHDPE/BF composite resulted in a more uniform dispersion of CCFA within the fiber-resin matrix. It was revealed that, from the SEM images, CCFA particles are well dispersed in the RHDPE/BF/CCFA composites, and the fiber is also well-embedded into the matrix. The results showed that the presence of CCFA prolongs the diffusion pathway, allowing for better dispersion of fillers in the composite. According to the SEM analysis, it is evident that the blend of BF and CCFA alters the physical structure of composite materials produced from natural fibers and recycled thermoplastics. Verma et al. [42] conducted SEM to investigate the morphology of pure HDPE and its composites with different CFA contents. The SEM images of unfilled HDPE represent a continuous single-phase field of morphology, whereas the images of HDPE/CFA composites represent the spherical nature of CFA particles, uniformly dispersed in the matrix. In addition, the images also depict the presence of grooves and extruded CFA particles that increased with CFA content. It was found that most of the extracted particles were significant, resulting in a poor contact interface between the CFA particles and the polymer. However, many small and high-surface area particles were found to be embedded in the polymer matrix. The homogeneous dispersion of CFA throughout the polymer matrix demonstrated the effectiveness of solvent-induced solubility blending as one of the methods for developing high-loaded CFA-based composites. According to the scanning electron microscope images, it

was found that the size of CFA particles increased with the CFA content, which may be attributed to the agglomeration process of CFA particles. Satapathy et al. [66] applied SEM to examine the interfacial adhesion morphology and fracture surface of RHDPE-JF-CCFA composites. The SEM analysis of the tensile fracture surfaces of the gold-coated samples substantiated that the JF and CCFA in RHDPE improved the adhesive interaction between the two surfaces and the matrix. Compared to the untreated JF-RHDPE, the matrix of the MAPE-treated JF-RHDPE showed less fiber pull-out, and the interfacial bonding between the fibers and the matrix was enhanced in the JF/CCFA-RHDPE composites. This behavior can be attributed to the increase in surface energy and the reduction of the interfacial tension by MAPE and CCFA, which leads to enhanced compatibility and adhesion between the fibers and the matrix. Moreover, the fracture surfaces of JF/CCFA-RHDPE composites were more cohesive and interlocked than those of JF-RHDPE and JF/MAPE-RHDPE composites, indicating better fiber-matrix bonding in the former composites. Patil et al. [67] observed compression-tested SEM images at a strain rate of 0.1 s-1 for both low and high magnifications of HDPE-CCFA composites. The micrographs did not reveal any significant differences in the morphology of fractured surfaces with respect to strain rate. The stress-strain curve indicated that the stress was almost uniform for all samples and strain rates, thus once again proving the fact that the deformation and densification properties were similar. Compression in synthetic foams was initiated by the collapse of the pores in the matrix, which is the cause of the initial densification. The fracture of CCFA caused further densification at higher strain levels. With increasing magnification, it becomes apparent that the deformed resin can be distinguished from the intact CCFA and its debris. The study concluded that the SEM analysis extracted the three-phase synthetic foams manufactured by 3D printing, which showed favorable sensitivity to strain rate. Alghamdi [68] used the SEM to evaluate the degree of interfacial adhesion between the OFA particles and the HDPE matrix. Cryogenic fracturing was employed to prevent any form of manipulation of the interfaces between the filler and matrix during the imaging process. The SEM images in Fig. 5 of the fractured surface in fresh and recycled composites indicated a significant interfacial adhesion between the filler and matrix in the former. Additionally, the HDPE matrices of the fresh composites exhibited thorough impregnation of the OFA particles even after the cryogenic fracturing process. The initial recycling process compromised the level of interfacial adhesion, resulting in a higher proportion of OFA particles becoming delaminated from the surrounding matrix. The OFA particles of comparable size were primarily concerned with preserving the uniformity of the filler/matrix adhesion. The interfacial adhesion between the filler and matrix remained unchanged in subsequent recycled composites. This finding supports the consistent tensile results observed across the first to fourth recycling periods. In general, using SEM imaging yielded qualitative data regarding the compatibility of the filler and matrix at the interfacial region, which is a pivotal aspect that governs the mechanical characteristics of composite materials.

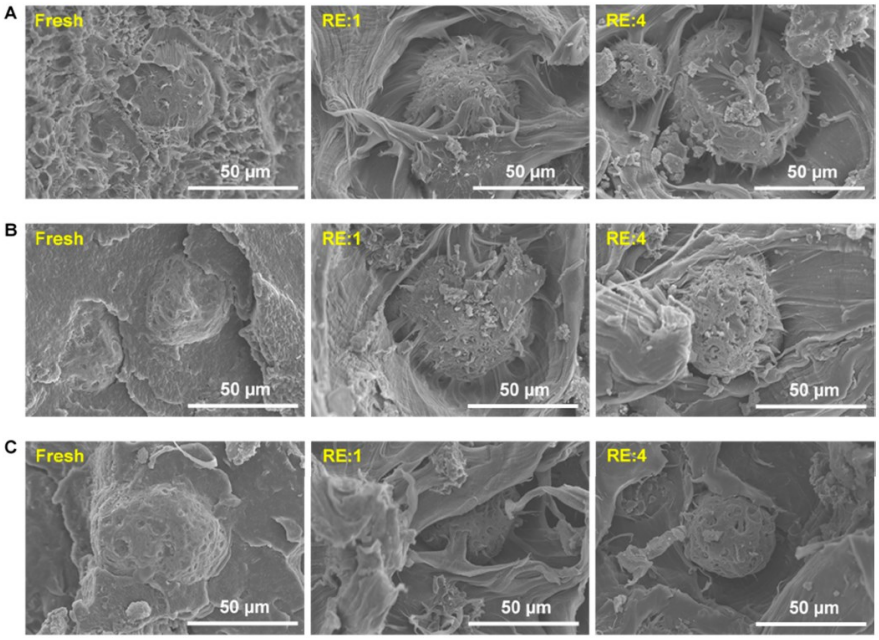

Fig. 5 SEM Micrographs of Cryogenically Fractured Recycled and Fresh Composites (A) OFA1-HDPE, (B) OFA2-HDPE, and (C) OFA3-HDPE [68].

Wu et al. [69] conducted a morphological study on the HDPE/CFA composites using SEM. The samples were cryogenically fractured in liquid nitrogen and then coated with gold before undergoing SEM study, which was conducted at an operating voltage of 10 kV. In the SEM study, it was found that the microscope surfaces of the untreated CFA particles are smooth, and they are spherical or irregularly shaped. In contrast, the surface of the treated CFA showed a non-uniform coating and appeared to have been successfully modified by 3-aminopropyl triethoxy silane. This modification was achieved via several events involving hydrolysis, hydrogen bond formation, and condensation between the silane coupling agent molecules. As noted from the SEM micrographs, the dispersion of CFA particles within the HDPE matrix was good, along with strong interfacial adhesion between the CFA and HDPE. The effect of the compatibilizer on this aspect was further studied through SEM analysis of morphology. It is observed that the distribution of CFA in an HDPE matrix is improved with the incorporation of a compatibilizer. The film coating on CFA particles may further enhance the mechanical properties. It was attributed to the reaction of the acid anhydride with amino groups in the modified CFA, forming a chemical bond that enhanced the interaction of CFA with HDPE. Stress concentration reduced agglomeration of CFA particles in the presence of compatibilizer. Similarly, the incorporation of excess CFA masterbatch (>15 vol.%) without a compatibilizer would result in the accumulation and poor distribution of CFA within the HDPE matrix, thus significantly reducing the mechanical properties of the manufactured composites. Alghamdi [70] investigated the morphological characteristics of the neat HDPE and HDPE filled with OFA composites. The study employed SEM to assess the surface degradation of the weathered samples and quantify the amount of FA particles exposed due to their long-term exposure to UV radiation. The cryogenic fracture technique was employed to expose the fracture surface of the sample interiors, which were then examined by SEM. SEM images were used to assess the extent of adhesion between filler and matrix. These images provided information about the quantitative measure of interfacial shear strength, which is one of the key factors controlling the mechanical properties of the hybrid system. SEM images of freshly prepared and aged samples, at 5 and 20 weeks, show that HDPE has intrinsic weather resistance. It can clearly be noticed that HDPE samples blended with organic fillers and additives, OFA/HDPE, revealed similar surface morphology after aging. SEM images revealed very little wear and crack formation at the surface of OFA/HDPE. The importance of the reduced impact of weathering can be comprehended by examining previous aging studies conducted on HDPE composites reinforced with other particles. The study revealed that the interface between the filler and matrix of composites with varying ages exhibited dissimilarities, while the texture of HDPE remained comparable at corresponding stages of aging. After 20 weeks of composite aging, multiple fractures were observed in the HDPE matrix phase. The pores exhibited various sizes, with the most extensive range measuring approximately 8-10 μm in diameter. The adhesion between OFA and matrix compensated for the degradation of properties caused by the matrix. The interfacial adhesion between the surrounding polymer matrix and various OFA/HDPE samples remained robust despite variations in FA concentration. The SEM images obtained from the samples aged 20 weeks revealed that the cryogenic fracture resulted in the exposure of FA particles. However, the pull-out mechanism involved the formation of a random layer of HDPE polymer on the surface of the particles. The superior mechanical properties of bulk composites were directly attributed to the high interfacial shear strength between the filler-matrix interfaces. Bin Nasir et al. [71] used the SEM equipped with Energy-Dispersive X-ray analysis (EDX) to analyze the microstructure of both the neat RHDPE and the RHDPE/RHA/CFA composite specimens. Their study compared composites made from 100% RHDPE, 90% RHDPE, and 80% RHDPE through a morphological analysis. They found that 100% RHDPE exhibits a limited number of voids featuring minute apertures, which suggests that the RHDPE underwent appropriate shredding. The elongated and necking broken surface of the specimen presents its ductility. The 90% RHDPE composite showed a honeycomb greyscale area, indicating the presence of RHA. The fractured surface area specimen did not show an elongated or necking morphology, indicating that the material is more prone to brittle fracture. In an 80% RHDPE composite, a honeycomb-like substance can be identified as RHA. More voids were seen compared to other composites. The presence of a huge void may affect the testing result of the specimen, as the adhesiveness and the filler-matrix bond will be compromised. The above problem can be obviated by using an extrusion apparatus during the amalgamation process, making the mixing of filler phase components and matrix phase material homogeneous and uniform.

3.1.2.Low-Density Polyethylene Matrix Composites

Khan et al. [72] studied the effect of the chemical modification of OFA on the morphological properties of LDPE composites.

FESEM was employed to investigate the dispersion of OFA particles in the polymer matrix. It was found that the OFA particles dispersed well in the polymer matrix; however, some accumulation occurred. However, better dispersion of OFA particles was observed after surface modification, and well-dispersed particles were visible at both high and low magnification with acid-functionalized OFA, i.e., acid functionalization of OFA improved the degree of dispersion, which is reflected in reduced aggregation size. The comparison of results for 2% OFA suggested a reduction of particle size by a factor of at least 2. Similarly, comparing 5% OFA loading results found improved dispersion due to surface modification. Figure 6 demonstrates the FESEM micrographs of the LDPE–OFA composite of (a) 2% OFA, (b) 2% COOH-OFA, (c) 5% OFA, and (d) 5% COOH-OFA. The study concluded that the COOH modification of OFA improved both the dispersion and rheological properties of OFA, and the concentration of the filler can be increased to 10% without compromising the properties of the composites. The uniform distribution of these tiny particles plays an essential role in enhancing the properties of the composites.

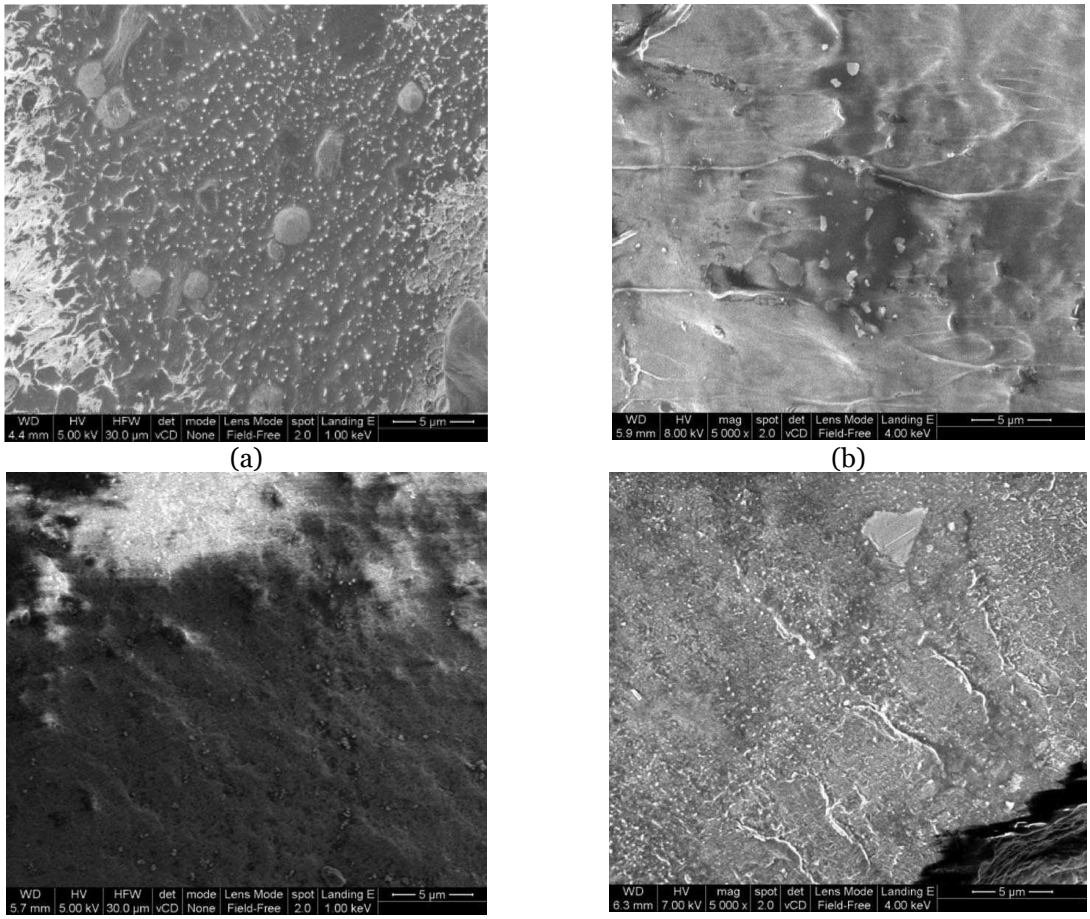

Fig. 6 FESEM Micrographs of LDPE – OFA Composite of (a) 2% OFA, (b) 2% COOH-OFA, (c) 5% OFA, (d) 5% COOH-OFA [72].

Dhawan et al. [75] examined the surface morphology of various samples and fractured Recycled Low-Density Polyethylene (RLDPE)-CFA/TPP composite tiles, which were analyzed using SEM. SEM images indicated that the CFA particles exhibited a spherical morphology, with diameters spanning from 20 nanometers to 2 micrometers. SEM images of the fractured surfaces of composite tiles made from plastic waste revealed that the plastic waste matrix, without any additives, exhibited roughness and deep flow patterns. Moreover, the SEM images of the composite tiles display an irregular surface featuring diverse pore sizes. The diminution of these pores is observed concurrently with the augmentation of the concentrations of CFA and TPP. The study revealed that the 20 wt.%. The CFA composite exhibited complete encapsulation of CFA particles within the plastic waste matrix, with a minimal flow pattern on the surface, indicating a favorable interaction between the matrix and CFA particles. The introduction of TPP with CFA particles decreased flow channels, suggesting that the two filler materials were entirely enclosed within the matrix. In general, using SEM analysis yielded significant findings regarding the morphology of the composite tiles

and the dispersion of filler materials within the matrix.

3.2.Transmission Electron Microscopy (TEM)

Over the last few years, considerable interest has been generated in the development of advanced composite materials for various industrial applications. Among these, FA-reinforced PE-based composites have received enormous attention due to their enhanced mechanical and thermal properties. In this respect, TEM has become one of the potent tools for retrieving detailed information about these composites, providing insight into their microstructural characteristics and interfacial interactions. This review aims to provide an overview of the TEM analysis techniques employed in studying PE/FA composites, highlighting the microstructural insights gained from these studies [78, 79]. TEM is a valuable tool for studying PE/FA composites in terms of morphology and structure at the nanoscale. Under TEM examination, high magnification can be achieved to reveal the microstructural features of interest, resulting in an extension of the dispersion of FA particles within the PE matrix, which is very important for obtaining information on interfacial interactions and the degree of particle aggregation. To that respect, it will contain agglomerates, interfacial voids, and defects that enable one to evaluate its structural integrity and possible mechanisms for failure of the composite material. In this respect, the study of the crystal structures in the PE matrix and FA particles can also be conducted with the help of selected area electron diffraction to determine crystallographic orientation, lattice defects, and phase transformations. [79, 80]. Satapathy et al. [62] studied the dispersion of CFA and CNFA in a WPE matrix through TEM. Investigations on the mechanical properties of CFA and CNFA-filled WPE composites under electron beam irradiation have been reported. It was found that CNFA particles dispersed well in the WPE matrix, and their morphology is more irregular as compared to that of the CFA particles, attributing to the better dispersion of CNFA particles in the WPE matrix, according to the study. Hence, electron-beam-irradiated composites exhibit better mechanical properties. Satapathy et al. [38] conducted TEM testing to investigate the dispersion of CNFA in the HDPE matrix of HDPE-CNFA nanocomposites. TEM images were taken for both the HDPE-CNFA and HDPE-irr. CNFA surfaces. The CNFA particles were found to be well-dispersed in the HDPE matrix, as indicated by the TEM images. The electron beam-irradiated HDPE-CNFA composite revealed a much more uniform dispersion of CNFA particles in the HDPE matrix than that of the particle size-reduced unirradiated composite. Satapathy et al. [63] presented TEM analysis to determine the dispersion of non-irradiated and irradiated CNFA in the WH blend matrix. It can be seen from the TEM images that the irradiated and non-irradiated CNFA agglomerated in the WH blend matrix. Due to the formation of agglomerates, the WH-CNFA and WH-irr.CNFA composites demonstrated relatively poor mechanical properties compared to the WH blend matrix. The findings showed that a uniform dispersion of the fillers within the matrix is essential for enhancing the mechanical properties of the composites. Khan et al. [64] reported the TEM analysis of the blends of HDPE, MWCNT, and UFFA. The TEM specimens of the blend composites were prepared by ultrasonication dispersion of composite powders in methanol. A few drops of the suspension were dropped onto a TEM support grid, which was a 300-mesh copper grid coated with carbon. The sample was then characterized under the TEM. In the nanocomposites containing 0.2% and 0.4% MWCNTs, as shown in the TEM micrograph, areas of higher electron density corresponded to the filler particles. The TEM image for the nanocomposite containing 0.2% MWCNTs is agglomerated and dispersed particles. Increasing the content to 0.4% MWCNT, the particles appear to cluster together; however, a combination of UFFA and MWCNT was found to be dispersed without clustering in some areas over the matrix. It is suggested that this agglomerated particle flow enabled stress transfer from the matrix to the filler, signifying an enhancement in interfacial bonding. Moreover, due to the fine size of the particles, they agglomerated and thus appeared as clusters in the TEM micrographs of UFFA. It has been suggested that adding MWCNT and UFFA into HDPE may potentially enhance the distribution of filler particles within the matrix, resulting in improved mechanical properties for such nanocomposites.

3.3.Thermal Properties

One of the most important techniques for evaluating the thermal properties and behavior of composites made from PE/FA is thermal analysis. The review provides a comprehensive understanding of the methods used in thermal analysis and, at the same time, provides valuable insights into the study of thermal stability, degradation mechanisms, and thermal conductivity of such composites. For composite materials that undergo high-temperature service, thermal stability is essential. The melting temperature, Tm, crystallization temperature, Tc, and heat of fusion can be measured using Differential Scanning Calorimetry, DSC, providing information about the thermal transitions the composite may undergo and the degree of its crystallinity. Thermogravimetric Analysis

(TGA) has primarily been applied to studies on the thermal stability and degradation behaviors of PE composites. Here, one measures weight loss as a function of temperature by heating the composite sample in an inert atmosphere at a controlled rate. The following parameters are obtained from this analysis, which includes the starting point of degradation temperature, rate of weight loss, and an overview of the thermal stability of the composite. Researchers have employed these various techniques to assess the mechanisms of degradation, thermal conductivity, and thermal stability of composites, aiming to gain a deeper understanding of these materials in terms of their thermal performance. These thermal properties would continue to play a vital in determining the suitability and performance of materials within industries, such as aerospace, automobile, and construction. Knowledge of PE/FA composites is, therefore, crucial for optimizing designs and applications [17, 42, 81].

3.3.1.High-Density Polyethylene Matrix Composites

Deepthi et al. [54] investigated the thermal analysis of the composites HDPE/CCFAs with the addition of a compatibilizer. The researchers investigated the thermal stability of such composites through TGA. The results showed that the commencement of thermal degradation for these composites occurred at a higher temperature than for neat HDPE, indicating improved thermal stability. It is worth noting that the introduction of a compatibilizer further enhanced the thermal stability of the resulting composites, as reflected by their reduced char formation and higher degradation temperature, which attributed to the enhanced interfacial interaction between HDPE and CCFA resulting from the surface modification of CCFAs and the addition of a compatibilizer. Baglari et al. [40] investigated the thermal properties of HDPE/CFA composites as a function of CFA loading between 0 and 70 vol.%. The transient hot wire method was used to measure the effective thermal conductivity, while the Coefficient of Linear Thermal Expansion (CTE) of these composites was evaluated using a Thermal Mechanical Analyzer (TMA). The TGA evaluated the thermal stability of the composites, revealing that the increase in CFA in HDPE enhances the thermal stability of the composite. The results showed that incorporating CFA in HDPE almost doubled the effective thermal conductivity. The improvement in the effective thermal conductivity of HDPE/CFA composites for high concentrations of CFA originates from the formation of conductive channels in the composites. The CTE of the composites was found to have a higher dependence on both filler loading and temperature, and the HDPE decreased by almost an order of magnitude when CFA was added. Besides, models were explored to predict the thermal conductivity of the composites; among them, the model proposed by Agari et al. [82] showed the best fit for the experimental data. The results suggest that the improved effective thermal conductivity and nearly an order of magnitude reduction in CTE caused by compositional variation in HDPE/CFA composites can be quite interesting for several applications, mainly electronic packaging, where CTE mismatch and heat dissipation are significant issues. It confirms that the interphase volume and strength of matrix-filler interactions are key parameters for predicting the CTE of polymer composites successfully. Satapathy et al. [62] orbited the combined loading of CFA and CNFA as fillers in WPE composites and their thermal characteristics in an irradiating environment using TGA and DTA. Based on these tests, several inferences can be drawn: Irradiation of the composites with electron beams improved their thermal stability. In contrast, both composites showed an increase in the onset degradation temperature (Tonset) and maximum degradation temperature (Tmax) with increasing irradiation dose. It can be seen, based on the results, that both filler type and amount have governed the thermal stability of the composites. The CNFA and CFA-filled composites exhibited enhanced thermal stability compared to the CFA-filled composites. The thermal conductivity increased with the increasing content of the filler. The CNFA-filled composites exhibited higher thermal conductivity than the CFA-filled composites. Satapathy et al. [38] studied the thermal properties of HDPE-CFA/CNFA composites using both TGA and DSC methods. The tests were conducted to examine the thermal stability and determine the behavior of the composite material under various conditions. The results showed that adding CFA/CNFA into the HDPE matrix increases its thermal stability. Weight loss and the corresponding derivative weight loss curves for neat and modified HDPE-CFA/CNFA composites clearly showed that modified composites exhibited better thermal stability throughout the temperature range. For this composite, the initial and maximum rates of thermal decomposition and the amount of residue left at 600°C were also analyzed. The results showed that the E-beam-irradiated CFA/CNFA composite had high thermal stability among the modified composites. It increased the chemical bonding inside the HDPE matrix, as CNFA acted as a nano-clay, thus enhancing thermal stability. Consequently, the improvement in bonding between the particles of CFA/CNFA and the

HDPE matrix increased, leading to a significant enhancement in thermal stability after electron beam irradiation. Not only that, but this enhancement in adhesion also restricted chain mobility and breakage to occur at higher temperatures, hence rendering it more thermally stable. In addition, the results from DSC indicated that the presence of CFA and CNFA in HDPE insignificantly impacted the melting behavior of HDPE. However, upon applying the MA grafting to the matrix, only a slight increase in the melting temperature was observed, which may be attributed to the improved adhesion between the matrix and the filler particles. Finally, the addition of CFA and CNFA may not have a significant effect on the thermal properties of the HDPE composite; however, modifications, such as electron beam irradiation, can significantly enhance their thermal stability. TGA and DSC tests revealed the different high-temperature applications of HDPE-CFA/CNFA composites. A further study by Satapathy et al. [63] explored the thermal behavior of WH-CFA/CNFA composites, which were studied using a TGA. In this process, the samples were heated from room temperature (RT) to 600 °C at a heating rate of 20 °C/min in a nitrogen atmosphere while recording the thermal degradation behavior. Their results proved that the developed composites had improved thermal stability by shifting both the initial and maximum degradation temperature towards higher values due to incorporating CFA/CNFA into the blend matrix. This behavior is attributed to the improved thermal characteristics of the fillers, which protected the polymer matrix from thermal degradation. Electron beam irradiation resulted in the most significant increase in thermal stability for all WH-CFA/CNFA composite modifications. The findings show that the irradiated WH-CFA/CNFA composite is a suitable engineering material for applications requiring both high strength and stiffness. This research indicates that these composites are serviceable at higher temperatures. Satapathy et al. [28] studied the thermal behavior of RHDPE/CF/CCFA biocomposites using DSC, TGA, and DTA thermograms. According to DSC analysis, the addition of CF increased the melting point and crystallinity of the composites. Upon the addition of 30 wt.% CF, the melting temperature of RHDPE/CF/MA-g-HDPE composites was raised from 132.5 °C to 139.5 °C. The TGA analysis showed that the addition of CCFA enhances the thermal stability of the produced composites. The ultimate decomposition temperature for RHDPE/CF/CCFA composites was increased relative to the RHDPE matrix. The improved thermal stability was due to MA-g-HDPE, which was found to couple with the CF hemicellulose and thus stabilize its structure, enhancing the overall thermal stability of the composite. Moreover, the DSC thermograms have also shown improved thermal properties in the composites in comparison to the RHDPE matrix. The study suggests that the developed composites can have potential as cost-effective and energy-effective wood substitutes for building applications and as a promising material for applications requiring good thermal stability. Khan et al. [64] presented the thermal properties of blends containing HDPE, MWCNT, and UFFA. The techniques used to study the thermal stability of the blends were TGA and DSC. TGA was performed under a nitrogen atmosphere using a thermogravimetric analyzer. Heating was conducted at a rate of 10 °C/min in an ambient temperature range of up to 350 °C with Al_2O_3 as a reference material. The results indicated that the presence of UFFA improved the thermal stability of the blends, which may be due to the ceramic nature of UFFA. The incorporation of 0.2% MWCNT significantly improved the thermal stability and char yield of the composite material compared to the material without MWCNT. The results indicated that the presence of UFFA reduced the crystallinity of the blends by 34.3%. Hence, it is conceivable that silane-treated UFFA interacted with the epoxy-functional compatibilizer, stabilizing the components of the blend that hindered the fine packing of the chains. The addition of 0.2% MWCNT slightly improved the crystallinity, although it remained lower than the pure HDPE. The results show that the combination of multi-walled carbon nanotubes and UVA in HDPE can improve the thermal properties of the resulting nanocomposites. Satapathy et al. [41] studied the effect of BF and CCFA reinforcement on the thermal properties of RHDPE composites. It was observed from the study that the addition of BF and CCFA to RHDPE composites altered the thermal properties of the composites. As shown in the DSC results, the incorporation of BF did not alter the crystallinity of RHDPE. However, it resulted in a significant decrease in the extent of crystallinity and Tc. The addition of CCFA to the RHDPE/BF composite resulted in a slight increase in Tm, suggesting that some interaction between the fibers/CCFA and the RHDPE matrix may have occurred. The TGA thermograms showed an improvement in the thermal stability of the fiber/polymer system with increasing CCFA addition. The results indicate that the addition of CCFA to the RHDPE/BF composite resulted in an increase in the residual mass compared to the RHDPE/BF composite. A decrease in the melt content and degree of crystallinity was also observed in this study, confirming the interaction between the fibers/CCFA and the

RHDPE matrix. BF and CCFA have been observed to affect thermal properties when incorporated into composites of natural fibers and recycled thermoplastics. These composites can be used in false ceilings, flooring, wood panels, and furniture, among many other applications, due to this. Verma et al. [42] studied the effect of CFA on the thermal properties of HDPE/CFA composites. The thermal properties were determined using TGA and DSC. TGA observed that the introduction of CFA increased the char residue of the composites, indicating improved thermal stability. The initial decomposition temperature, IDT, and mass loss of the composites increased by approximately 15 °C and 5 °C, respectively, with increasing CFA addition up to 25 wt%. The improved thermal stability of these composites is associated with the inert metallurgical properties of CFA. These properties enable efficient heat transfer/dissipation in the composites, preventing or delaying the local heat accumulation and the accompanying decomposition processes. It is observed from DSC the analysis that the addition of CFA did not affect the melting and crystallization behaviors of HDPE. The maximum endothermic temperature, standard melting temperature, and heat of fusion of HDPE/CFA composites were found to be similar. Hence, the use of CFA insignificantly affected the mentioned parameters, whereas research studies concluded that the addition of CFA to HDPE/CFA composites resulted in higher thermal stability responses. The results showed optimum diffusion in high-temperature applications. Satapathy et al. [66] evaluated the thermal properties of JF/CCFA-reinforced RHDPE composites by TGA and DSC. From the TGA and DTG curves obtained for various composites, it was observed that the onset of decomposition of RHDPE started at around 461 °C. However, the maximum temperature at which decomposition occurred was 484 °C. The incorporation of JF and CCFA in the RHDPE matrix slightly reduced the decomposition onset temperature, indicating a decrease in the thermal stability of the composites produced. A decrease in the maximum decomposition temperature values was observed with the incorporation of JF and CCFA into the composites, thereby decreasing their thermal stability. The DSC results show that the RHDPE matrix has a slightly higher melting peak at 134.33 °C with higher enthalpy values than its fiber/filler composites. The decrease in the melting temperature values of the composites upon incorporation of JF and CCFA indicates a decrease in their crystallinity. The presence of MAPE in the composites reduced the melting temperature of the JF-RHDPE and JF/CCFA-RHDPE composites, indicating that crystallization occurred faster to eventually form smaller crystals. The results show that the incorporation of JF and CCAF can be highly effective in modifying the thermal performance of RHDPE composites. Therefore, it can be wise to carefully select the weight percentage of JF and CCFA used in these systems to avoid decreasing the thermal stability and crystallinity of these composites. Alghamdi [68] studied the thermal properties of OFA/HDPE composites, which were evaluated by TGA and DSC. To study the degradation properties of fresh and OFA-blended HDPE and HDPE samples, TGA analysis was performed. The samples were annealed against a temperature gradient from 25 °C to 600 °C at a heating rate of 5 °C/min. The experiments were conducted in an airborne environment to replicate the degradation of the polymer by the melting process. The weight loss of the HDPE sample was noticeable at approximately 275°C and was completely degraded at approximately 510°C. In direct comparison, the thermal degradation in the polymer component of the OFA/HDPE samples reached about 90% at 510°C, while the OFA particles remained undamaged. The main reason behind this behavior was that the metal particles in the OFA component have ideal thermal stability. TGA was used to investigate the degradation behavior of the composites around the temperature at which they were processed. From the results, it is evident that thermal decomposition was not prominent in all samples subjected to melt processing within the temperature range of 220-240 °C, indicating that this temperature range is safe for preparing high-value polymer composites. DSC analyses were performed to determine the crystallinity developed by the recycled materials. The melting temperatures of the freshly prepared samples were slightly higher than those of the remelted samples, which may be due to the lower crystalline fractions in the HDPE matrices. However, the remelted samples showed hardly any clear melting peaks, which may indicate that these materials can be recycled multiple times without significant loss of polymer crystallinity. The degree of crystallinity was estimated with respect to the melting heat obtained by a perfect polyethylene crystal without defects. The result showed that the degree of composite crystallinity remained constant for all recycling stages, and OFA1/HDPE composite samples experienced the least deviation from this value. This uniformity in particle dispersion may provide a uniform crystalline orientation within all composite samples. Wu et al. [69] investigated the thermal properties of HDPE/CFA composites. The thermal stability analysis of these composites was performed using TGA. Pure HDPE had an initial decomposition temperature of 390 °C and a maximum

decomposition temperature of 514 °C, based on the TGA results. The addition of CFA masterbatch to HDPE enhanced the thermal stability of the resulting composites. The HDPE-5% CFA masterbatch composite initiated thermal decomposition at 220.8 °C, reached a maximum thermal decomposition temperature of 571.75 °C, and generated 2.1% carbon during the process. When the CFA masterbatch content increased to 20%, the IDT of the composite became 221.93 °C. Besides, the thermal decomposition showed a stable trend at 568.05 °C, with a carbon formation rate of 8.0%. Analysis of the TG and DTG data for the composites showed that the thermal decomposition peak of all composites was higher than that of pure HDPE. This research showed that the inclusion of CFA masterbatch into HDPE enhances the thermal stability of the composites. From the TGA results, it can be observed that the onset and maximum decomposition temperatures of the composites are higher than that of pure HDPE. The TGA results also showed a significant effect of adding a compatibilizer on the thermal stability of the composites. Among other things, the 10% CFA masterbatch with 5% compatibilizer showed that IDT was 222.5 °C, while its maximum decomposition temperature was found to be 571.5 °C corresponding to a 2.5% carbon composition, indicating that increasing the proportion of compatibilizer, mainly from 5% to 15%, reduced the initial and maximum decomposition temperatures of the respective composites by about 2.5% and 1.5%. The observed phenomenon could be due to the overfeeding of the compatibilizer, which resulted in the fragmentation of the highly crystalline morphology of HDPE and increased the flexibility of the composites. Consequently, the thermal stability of the composites was reduced. The effect of the compatibilizer was observed with respect to the thermal decomposition behavior of the composites. As a result, the TGA curves indicate that the addition of a compatibilizer causes a significant shift of the peaks related to the thermal decomposition of the composites towards higher temperatures. The results showed that the presence of a compatibilizer improves the interface adhesion between the filler particles and the HDPE matrix, which improves the thermal stability and delays the thermal decomposition. Alghamdi [70] studied the thermal properties of pure HDPE and OFA/HDPE composites using TGA. Using TGA, one can analyze the processing temperature, decomposition behavior of the formed samples, and FA content of HDPE. Tests were performed in the air to simulate the environmental conditions that develop during the melting and high decomposition process of the polymer. The results showed that the weight loss of all samples began at approximately 280 °C, and decomposition was completed at around 600 °C. A direct relationship was observed between the amount of fillers and the thermal stability of the composite samples. The main causative factor for this behavior was the high thermal durability of the mineral microparticles inside the highly filled OFA samples. At a temperature of about 500 °C, the weight degradation was found to vary by about 5%, indicating the presence of FA fillers within the range of 5-15 wt.% in steps of 5 wt.%. It was found that the homogeneity of filler concentration became critical when the composite material was exposed to UV radiation and weathering for an extended period. The results showed that significant polymer degradation occurred after 20 weeks of aging and that additional UV exposure would have led to premature failure of the material. The study also showed that the adhesion of the filler matrix, which governs the shear strength between the composite system's surfaces, was a direct factor in determining the composite's mechanical properties.

3.3.2.Low-Density Polyethylene Matrix Composites

Khan et al. [48] studied the effect of OFA loading and functionality on the thermal properties of LDPE composites. Insignificant effect of OFA was observed on the melting point, onset temperature, and peak crystallization. The crystallinity (Xc) of the composites was evaluated by DSC. Xc was determined from the heat evolved during crystallization, ΔHc, by the relationship: Xc% = ΔHc/(1-wt%)/ΔHm, where ΔHm is the heat of fusion of 100% PE crystal and wt.% is the weight fraction of OFA in the composites. In the study, the heat of fusion value of 290 J/g PE crystal was used. OFA changed the onset temperature of crystallization without affecting the peak temperature. The study provides valuable information on the effect of OFA loading and functionality on the thermal properties of LDPE composites, which can be highly beneficial in developing high-performance and sustainable materials. Adeosun et al. [73] studied the DSC curves of LDPE-CFA/CC samples at various scan rates of 5, 10, 15, and 20 °/min. The samples were heated to 200°C, then cooled to the minimum temperature, and subsequently reheated to 200 °C again. The curves contain endothermic peaks; however, crystallization and transition peaks were not observed in this study. Furthermore, the curves did not depict any significant melting heat, and the peaks were not well-defined, which may be due to the strong influence of CC additives on the polymer structure. These additives disturb the crystalline structure of the polymer, making it highly amorphous. Another observation was that as the scan rate increased, the peak

temperature also increased. These results suggest that the addition of CFA/CC hybrid filler to LDPE will produce a material with a high degree of amorphous, which may impact its properties and, thus, potential application areas. Porabkaet al. [74] studied the effect of filler content and CFA granulation on the thermal behavior of LDPE and CFA composites. Thermal analysis of LDPE + CFA samples was performed using DSC and TGA methods. It was found that the melting point of pure LDPE was 115 °C. The temperature at which the polymer decomposition processes started was around 400 °C. The first effect was observed at approximately 394 °C, accompanied by a slight decrease in mass. The second endothermic effect, resulting from heat absorption and mass loss, appeared suddenly. By 500 °C, the polymer had completely melted. The results showed that the addition of CFA to the polymer blend insignificantly changed its melting point, indicating that the crystalline structure of LDPE was intact. In samples with CFA greater than 15 µm, small increases in Tm meant better thermal resistance of these materials. The larger the sample size, the better the thermal resistance, resulting in the most considerable noticeable difference in the polymer decomposition area. Specifically, the small melting peak at 394 °C decreased when 5 wt.% of the 15–30 µm CFA fraction was added and completely disappeared in the composite containing 5 wt.% of the larger 30–60 µm particles. The temperature at which the composites started to decompose (without bulk) was about 20 °C, i.e., higher than that of pure LDPE. These results demonstrate that CFA can be used to increase the thermal resistance of LDPE-based composites, and the size of the CFA particles plays a crucial role in determining the thermal behavior of the composite. Dhawan et al. [75] investigated the thermal properties of RLDPE-CFA/TPP composite tiles. RLDPE showed a very moderate weight loss of approximately 7% at an onset temperature of 300 °C. Samples loaded with 20 wt% CFA showed a weight loss of approximately 1% at this temperature. The same was true at 300 °C, which means that the introduction of TPP did not affect the thermal stability of the composite tiles. However, increasing the TPP content from 1% to 5% increased the ash residue of the tiles from 21.7% to 27.3%. TPP reduces the linear combustion rate and increases the combustion temperature, which could potentially lead to an increase in the ash residue of the composite materials. The thermal stability of the composite tiles was investigated using TGA. These composite tiles showed stability up to a temperature of about 700 °C. Thus, TGA was useful in measuring the weight loss, due to both decomposition and volatile matter, identifying impurities, and calculating the percentage composition of fillers and matrix in composites. According to the TGA of composite tiles, the incorporation of CFA particles showed a stabilizing effect on thermal decomposition. It was also demonstrated that metal hydrogels contained thermally stable metal oxide particles, such as TiO_2 and Al_2O_3, which also stabilized the thermal decomposition. The investigation results into the thermal properties revealed “solid thermal stability and low flammability” for this class of composite tiles.

3.4.Physical Properties

3.4.1.Density Measurement

The performance improvement by controlling the density of a PE composite with FA as a reinforcing constituent is a complex approach. Understanding the interrelationship between FA content, processing conditions, and resulting density enables balancing material cost with weight reduction in relation to the required mechanical properties of the material. Different processing techniques, therefore, impact significantly on the density and performance of the ensuing PE-FA composites. The parameters of melt mixing, such as temperature and shear rate, and compaction methods may also modify FA dispersion and interfacial adhesion, thus ultimately impacting packing efficiency and density. Besides, compaction methods—for instance, compression molding or extrusion methods—can affect the formation of porosity and voids, which in turn influence the final density and associated properties. Understanding the relationship between density and other properties is crucial in material design [83, 84]. Concretely, the addition of a moderate content of FA enables the material to achieve increased stiffness and strength while maintaining a lower density than neat PE. Hence, it will be of great importance to applications requiring lightweight materials. If, on the other hand, the opposite purpose is intended—minimum density in thermal insulation—then the emphasis should be on increasing the FA content and purification techniques, even if it risks the mechanical strength in some measures. Density measurements for composites made of FA-PE are not mere single values; they represent crucial indicators for material efficiency and the potential of its performance. Therefore, with appropriate observation and careful analysis of the complex relationship between the FA content, processing conditions, and the resulting density, the full potential of these sustainable composites can be realized, as a result, expanding their scope of applications in various industries [84, 85].

3.4.1.1.High-Density Polyethylene Matrix Composites

In the study conducted by Chand et al. [56], the density of CCFA-filled HDPE composites was measured using a precision balance and Archimedes principle. It has been reported that the density of the composites decreased with increasing weight concentration of CCFAs. The pure HDPE had a density of 0.953 g/cc. The density values obtained for the untreated CCFA composite with the lowest and highest weight concentrations of CCFAs (10 and 20 wt. %) were 0.83216 and 0.72067 g/cc, respectively. In comparison, the silane-treated CCFA composite with the lowest and highest weight concentrations of CCFAs (10 and 20 wt. %) had densities of 0.88797 and 0.78699 g/cc, respectively. It was also revealed that the density of the composites was improved significantly with silane-treated CCFAs. The main reason behind the observed density reduction with increasing filler concentration is the low density of the CCFAs used. The densities of the CCFAs were found to be less than 0.7 g/cc, which is significantly lower than the density of the polymer matrix. Kumar et al. [13] reported the results of density measurements conducted on HDPE and the syntactic foam composites filled with untreated and silane-treated CCFA. Computed densities were compared with theoretical predictions made by the rule of mixtures. The CCFA breakdown during its manufacture seems to be responsible for the discrepancy in density values between the theoretical and experimental measurements. HDPE syntactic foams with 66.4 vol.% filler loading reflect the maximum CCFA breakage for both treated and neat components. When the filler content increased, the particle-to-particle contact also increased, and the mix viscosity was reduced. The filler particles have increased the fracture rate accordingly. In the case of treated details, a higher rate of breakage of CCFA particles has been reported. HDPE and CCFA have been interfacially bonded and hence are highly compatible. It means that the density of fractured particle fragments was about 3.5 g/cc. Furthermore, since samples lacked matrix porosity, higher density values were indicative of CCFA fracture.

3.4.1.2.Low-Density Polyethylene Matrix Composites

Chand et al. [55] investigated the effect of untreated and silane-treated CCFAs on the density of LDPE composites. The measured density value for LDPE fell between 0.910 and 0.940 g/cc, which may be attributed to less tightly packed CH_2 molecules and low crystallinity. The density of the CCFAs was very low (<0.7 g/cc), so their incorporation in LDPE reduced the overall density for both CCFA and silane-treated CCFA. The density values ranged from 0.8624 g/cc down to 0.8386 g/cc for the 10 and 20 wt.% composites of the untreated CCFA, respectively. The values ranged between 0.8592 g/cc and 0.8354 g/cc for 10 and 20 wt.%, respectively, for silane-treated CCFA. The lowest density composite was 20 wt.% silane-treated CCFA, whereas the one with the highest density was 10 wt.% untreated CCFA. Incorporating silane-treated and untreated CCFA in LDPE reduced density with an insignificant treatment effect. A reduction in the density of such composites could be important in applications where lightweight materials are required. Another study, conducted by Adeosun et al. [73], investigated the effect of CC and CFA hybrid filler particles on the density of LDPE composites. In this work, these composites were prepared using the melt casting method with variations in the weight percentages of CFA and CC. The results showed that the density of the LDPE composite increased with the weight percent of CFA in the hybrid filler, up to an optimum composition of 20 wt.% CFA and 30 wt.% CC, which ensured the highest density. Otherwise, a rise in CFA content resulted in a decrease in density, while CC increased, which is attributed to the fact that CFA has a lower density of 0.8–1.0 g/cc than CC, which has a density of 2.7 g/cc. However, the combination of both fillers is required to be combined for optimum density. The reasons for the increase in density can be attributed to the higher density of CFA in comparison to CC. The study contributes valuable information on the use of hybrid fillers for enhancing the physical properties of LDPE composites. Dhawan et al. [75] studied the density measurement of RLDPE-CFA/TPP composite tiles. It was observed that the bulk density value of the waste plastic RLDPE was 0.93 g/cc. In addition to CFA particles in the composite tiles, a marginal increase in bulk density from 0.93 to 1.0 g/cc was observed, accompanied by an increase in the CFA content from 0 to 20 wt.%. The increase in density can be explained by the difference in densities between RLDPE and CFA's. Similarly, the density of the samples was not significantly altered by the addition of TPP content from 1% to 5%. It was found that the density of the different composite tiles ranged from 0.989 to 1.02 g/cc. The marginal increase in density with an increase in CFA content could have been attributed to the differential between RLDPE and CFA.

3.4.2.Water Absorption Measurement

While PE is one of the most used polymers due to its flexibility and relatively cheap cost, it does have some inherent hydrophobic properties. Still, with FA, one of the byproducts of fuel combustion, as reinforcement, hydrophilic elements are introduced and hence affect the behavior of water absorption, which is a complex process influenced by several aspects,

including the qualities of the FA-reinforced composites, the manufacturing procedures, and the composition of the composites. According to research, there is a primary increase in water absorption with FA content [86, 87]. Micropores and hydroxyl groups in the ash particles are responsible for this behavior. However, some studies have examined this assumption because the increasing filler content in a composite material may be responsible for an eventual "saturation effect" at higher loadings. There is a likelihood that the increased filler content may act against water ingress by creating tortuous paths and possible denser packing. Moreover, several processing methods that utilize silane coupling agents further enhance the potential adhesion of the FA to the PE, potentially blocking the capillary channels of the FA and thus reducing the input of water. Hence, these complex relationships must be understood and considered when creating composites for applications under more rigorous water-resistance conditions, such as in water-based structures or pipes. Further research is required to optimize water absorption fully and to achieve potential sustainable composites by investigating the interplay between FA properties, processing parameters, and surface modification strategies [87, 88].

3.4.2.1.High-Density Polyethylene Matrix Composites

The water absorption characteristics of RHDPE and its composites with CF and CCFA were examined by Satapathy et al. [28]. Due to the hydrophilic nature of CF, the tendency for water absorption of the RHDPE/CF composite system was reported to be more progressive than the RHDPE/CF/MA-g-HDPE composite system. However, introducing MA-g-HDPE as a compatibilizer in the RHDPE/CF composite system enhanced the interaction and reduced water absorption. The fiber-matrix adhesion was increased with the presence of MA-g-HDPE dispersed between the CF and RHDPE matrix and, hence, improved the water resistance capacity. There was a drastic decrease in the percentage of water absorption with the addition of CCFA into the RHDPE/CF/MA-g-HDPE composite. This behavior is due to the cavities in the CF and the RHDPE matrix being filled with the CCFA, which hinders the penetration of water into the composite beyond a particular limit. Thermoplastic composites reinforced with CF, due to their low cellulose and high lignin content, have been found to exhibit excellent water resistance compared to other natural fibers. Satapathy et al. [41] investigated the effect of BF and CCFA reinforcement on the water absorption of RHDPE composites. It was reported that the water absorption of composites comprising RHDPE and BF, as well as those composites comprising RHDPE, BF, and CCFA, increased linearly with immersion time. The incorporation of MA-g-HDPE in the RHDPE/BF composite has enhanced interfacial adhesion and reduced water absorption, which was further reduced upon the introduction of CCFA filler in the composite. From the study, it was shown that the RHDPE/BF composite exhibited a higher water absorption propensity compared to the RHDPE/BF/MA-g-HDPE composite. The presence of CCFA in the interstice of both fiber and matrix hindered the penetration of water into the inner part of the composite. It is also found that CCFA results in a longer diffusion pathway, thereby reducing the rate of water absorption. Satapathy et al. [66] investigated the influence of JF and CCFA on the moisture stability of JF-RHDPE and JF/CCFA-RHDPE composites in the presence of MAPE through the water absorption test. The obtained results indicated that the absorption of water increased linearly, with a similar trend for all specimens. It was found that the prepared composite samples of JF-RHDPE showed a greater tendency to absorb water, which may be attributed to the hydrophilic nature of JF. In the JF-RHDPE system, the MAPE coupling agent served as a dispersant agent in separating the fiber and matrix components, thereby reducing the rate of water absorption. The water absorption in the JF/CCFA-RHDPE composites was reduced due to the long diffusion paths created by the CCFA embedded within the JF-RHDPE matrix compared to the fiber-filled RHDPE composite systems. The results have shown that CCFA could be an ideal component for making the JF-RHDPE composite material with improved moisture stability.

3.4.2.2.Low-Density Polyethylene Matrix Composites

Adeosun et al. [73] studied the water absorption rate for the LDPE-CFA/CC composite. It was observed that composites with an increased CC content showed increased water adsorption. By contrast, the composites having a higher CFA content tended to exhibit a decreased adsorption rate. Although CFA contains high amounts of silica and is, therefore, likely to impart some degree of hydrophilicity, the findings clearly showcased CC's excellence in hydrophilicity. The authors proposed that this may be because CC filler is hydrophilic, and therefore, it attracts water molecules, leading to increased water absorption. Furthermore, it was reported that as the soaking time increased, the rate of water absorption for all composites also increased. The weight percentage of CC in the composite impacted the LDPE-CC/CFA composite regarding water absorption rate. Such information would be useful in understanding the behavior of the composite in contact with water under service conditions.

Dhawan et al. [75] investigated the water absorption properties of RLDPE-CFA/TPP composite tiles. After seven days, the samples were removed, washed with distilled water, and then dried. The weights and dimensions of the samples were recorded and compared to the original weights and measurements. From the results, it can be seen that the water absorption of each sample was approximately the same, with a water absorption rate of 0.06%. The results suggest that the addition of CFA particles and TPP content insignificantly affected the water absorption characteristics of the composite tiles. The absence of any remarkable change in weight and dimensions suggests that the composite tile has good water resistance characteristics.

3.4.3.Rheological Properties

The rheological performance of the FA-reinforced PE composites has been an area of immense interest in material science. Rheology is a branch of physics that mainly focuses on studying the flow and deformation of matter; therefore, it holds significance in explaining the dynamic behavior of these composites. The incorporation of FA, a byproduct obtained from fuel combustion, into PE matrices as a reinforcement material results in significant changes to their rheological characteristics. In this process, the viscosity of PE composites will be different after incorporating FA particles. FA particles are characterized by a wide distribution in terms of shape and size, resulting in a very significant interaction with the polymer matrix [42, 72]. This behavior ultimately affects the flow behavior of the composite material, indicating that factors, such as particle size, particle loading, and distribution within a polymer matrix, affect the viscosity of the composite. Viscosity in these composites is crucial for controlling and understanding processing techniques such as extrusion and injection molding. The addition of FA into a composite material can strengthen the PE matrix, having a significant impact on the viscoelastic properties. The elastic, storage, and loss moduli of composites are remarkably influenced by FA particles. Interaction at the particle-matrix interface of the polymer contributes to the overall mechanical behavior of the composite. In summary, viscoelastic properties are highly relevant to composite materials used in applications where resistance to deformation and stress is desired, such as in structural components or packaging materials. [42, 89]. In the case of FA-reinforced PE composites, rheological behavior is influenced by both temperature and shear rate. Temperature changes alter the viscosity of the melt and the degree of particle dispersion in the polymer matrix, thereby changing the flow behavior. The shear rate can cause changes in the orientation and alignment of FA particles, and hence altering the rheological response. These external factors' effects, therefore, need to be understood to predict composite behavior under different processing and application conditions for controlling the same. Detailed knowledge of rheological properties is, therefore, necessary to improve processing techniques and enhance performance in various applications. Further studies and development in this area will undoubtedly lead to the creation of sustainable materials with enhanced functional properties. [42, 72, 90].

3.4.3.1.High-Density Polyethylene Matrix Composites

Adeosun et al. [73] examined the MFI of the polymer composite, which was evaluated using a self-made melt flow indexer with a piston diameter of 9.5 mm. According to the research, the addition of the hybrid filler of the CFA/CC ash reduced the MFI of the composites. It is, however, recorded that an increase in the wt. % of CFA significantly affected reducing MFI compared to the increase in CC content. It is also observed that at higher CC contents, the composites had a larger MFI, while at higher quantities of CFA, the composites had a lower MFI. The study concluded that the reduction in MFI was indicative of a decrease in the plasticity and processability of the polymer resulting from the addition of CFA. On the other hand, CC addition may increase plasticity and processability in the polymer. A low MFI was found to improve the mechanical properties and thermal stability of the system. It means that the type and amount of the filler used in the composite must be such that the desired MFI and mechanical properties are achieved. Verma et al. [42] investigated the rheological behavior of HDPE/CFA composites by measuring MFI and capillary rheometry. The composites revealed lower MFI than pure HDPE, with the trend being inversely proportional to the content of CFA. This observation might be attributed to the fact that CFA particles function as a physical cross-link, which has an effect on the polymer chains. Results of capillary rheometry analysis proved that the processability and viscosity of HDPE composites were significantly affected by the use of CFA during their processing. For both composites and pure HDPE, non-Newtonian behavior was observed within the studied range of shear rates, and it was considered to be a shear-thinning effect since the viscosity decreased with increasing shear rate. This shear-thinning behavior can be explained by the orientation of the polymer chains in the direction of the flow, which decreased the viscosity of the molten composite. The increased shear viscosity observed with the incorporation of CFA could be attributed to a shift from fluid-like to solid-like rheological behavior. This phenomenon is attributed to the

hindrance caused by the filler particles, acting against the movement of polymer chains. The research findings revealed that the incorporation of CFA significantly influenced the rheological characteristics of HDPE/CFA composites, making them suitable for various processing methods.

3.4.3.2.Low-Density Polyethylene Matrix Composites

Khan et al. [72] investigated the effect of the chemical modification of OFA on the rheological properties of LDPE composites. Rheology analysis was performed using a controlled strain rheometer, while dynamic shear tests were performed in cone-and-plate geometry. The results indicated that the addition of uniformly dispersed OFA particles to a polymer matrix changed the behavior of the polymer from liquid-like to solid-like, increasing its viscoelastic properties. It can be observed that both the storage and loss moduli increased with an increase in the loading of OFA. The effect was predominant at low frequencies, suggesting "pseudo-solid-like" behavior. The addition of the compatibilizer PE-grafted-Maleic Anhydride (PE-g-MA) improved the rheological behavior of the composites. The filler concentration can be increased up to 10% with no adverse effect on the properties of the composites.

3.4.4.Aging Studies

The aging behavior of FA-reinforced PE composites is thus a complex process in which the content of FA, processing conditions, environmental exposure, and interfacial interactions all intervene. While FA can offer extra initial mechanical properties and reduce costs, its long-term influence on aging remains of importance to study. In this context, the FA content is the most important factor, according to studies, and moderate loadings of 10–15 wt.% may demonstrate better resistance to both thermal and UV degradation compared to neat PE [70, 91, 92]. It is likely that the reason this filler material is so effective is due to its efficacy in scavenging free radicals and blocking light penetration. However, increasing the content of FA can lead to microcracking, further moisture ingress, and additional deterioration. For example, processing methods involving silane coupling agents can improve adhesion between FA and polymer and reduce the aforementioned negative effects. The mechanisms of FA-polymer interaction under various aging conditions need to be understood to optimize such composites for sustainable and durable applications [92, 93].

3.4.4.1.High-Density Polyethylene Matrix Composites

Satapathy et al. [62] investigated the impact of air aging on the tensile properties of CFA/CNFA-filled WPE hybrid nanocomposites. The results revealed that the tensile properties of the aged samples were higher for CFA- and CNFA-filled WPE composites subjected to electron beam irradiation. This result, therefore, indicates that electron-beam irradiation enhanced the aging resistance of the composites. The improved aging resistance may be attributed to the cross-linking of the polymer matrix due to irradiation, resulting in a three-dimensional network structure. Cross-linking prevented degradation of the polymer matrix during aging, maintaining higher retention of tensile properties. Satapathy et al. [38] investigated the aging effects on HDPE-CFA/CNFA composites. The percentage retention of tensile strength and elongation at break were analyzed before and after aging. The aging studies showed that the tensile properties of the aged samples were affected by exposure to high temperatures and prolonged periods. Specifically, there was a decrease in both the UTS and elongation at the break of the aged samples compared to their unaged counterparts. Besides, the results showed that the HDPE-CFA/CNFA composites with irradiation exhibited higher retention of tensile properties than the unirradiated composites. A further study by Satapathy et al. [63] investigated the aging of WH-CFA/CNFA composites. The tensile properties before and after the aging of the composites were measured, and the percentage retention of tensile strength and elongation at break was calculated. The results indicated that the addition of CFA/CNFA to the WH blend matrix increased the percentage retention of tensile strength and elongation at break after aging. The concentration of fillers has an inverse effect on elasticity and deformation ability, hence reducing the matrix absorption of deformation energy. It was observed, however, that electron beam irradiation of WH-CFA/CNFA composites resulted in the highest percentage retention of tensile strength and elongation at break among all the modifications. The cross-linking, resulting from the irradiation process, improved the resistance of the composites to air aging. In contrast, the elasticity of the material decreased with an increase in the filler concentration. These results indicate that irradiated WH-CFA/CNFA composite will be a suitable engineering material for applications requiring very high air aging resistance. Alghamdi [70] investigated the effect of natural aging on the mechanical properties of pure HDPE and OFA/HDPE composites. As expected, results indicated that the natural aging process caused significant changes in Young's modulus for pure HDPE material. However, the results for the OFA/HDPE samples were very promising, with a relatively low loss in modulus during the aging process. This remarkable result is attributed to the

stabilizing effect of FA fillers by absorbing light across the entire solar spectrum, preventing the penetration of high-energy photons into the surrounding polymer matrix, thus limiting the degradation of the polymer. Another aspect considered was the influence of the aging process on the tensile strength of HDPE and OFA/HDPE. According to the findings of this study, there was a progressive loss in tensile strength with an increase in the percentage of filler during the aging process. The interfacial morphology of the fillers and matrices in the aged composites was determined using SEM. Concluded here, polymer degradation was similarly intense for all samples since they were based on the same grade of HDPE precursor. In this micrograph, the interface between the filler and matrix was visibly different in composites of different ages. However, the texture of HDPE remained the same at equivalent aging steps. Fractures were observed to have occurred at several points within the HDPE matrix phase when the composites were aged for 20 weeks. A presence of pores of varying different sizes was noted, with the widest size range being around 8-10 micrometers. In this case, as in other polymer composites, the improvement in mechanical properties was mainly due to the filler-matrix adhesion, which compensated for the loss in properties resulting from matrix degradation. The interfacial adhesion between the polymer matrix and the OFA/HDPE samples remained intact with varying concentrations of FA.

3.4.5.Flammability Test

Composites of FA-reinforced PE have generated keen academic and industrial interest in their flammability properties. This new composite material combines the excellent mechanical properties attributed to FA with the intrinsic fire-resistant characteristics that FA possesses, so it is very promising for applications where improved flame retardancy is required. Such flammability behavior in these composites is the result of combined effects by the PE matrix and the FA filler. The first role of the FA particles is to act as heat sinks by dissipating heat energy and thereby delaying ignition. The second role of FA in the combustion process is the promotion of a protective char layer, which will then behave like a barrier, which dampens the spread of flames and reduces heat and mass transfer. Lastly, the FA particles help form a compact and stable char structure, thus making the composite more resistant to thermal degradation. The flammability characteristics of PE reinforced with FA composites can be modulated by varying the filler loading, particle size, and distribution within the matrix. This behavior thus offers a versatile method for achieving specific levels of flame retardancy. Further research is required to uncover the key underlying mechanisms controlling flammability behavior in these composites, which will enable the optimization of their formulation for specific applications where fire safety is of the utmost importance [94, 95].

3.4.5.1.Low-Density Polyethylene Matrix Composites

Porabka et al. [74] investigated the impact of the filler content and granulation of CFA on the flammability of composites prepared from LDPE and CFA. They concluded that polymers always burn consistently: when heated by a flame, they release heat, break down, and emit gaseous hydrocarbons into the surrounding area. When these gaseous hydrocarbons are heated enough, they cause a higher output of heat. This process continues until all the polymers are completely decomposed. The incorporation of CFA into LDPE transforms the polymer, thus producing less flammable gases, suppresses the flame, or even quenches it and reduces the feedback heat from the flame to the degrading polymer-all of which suppress combustion. Through experiments conducted using fire, it was confirmed that introducing CFA into LDPE reduced burn. The flow had been successfully monitored at temperatures exceeding 150 °C. Upon a closer examination of the composite films after the experiment, it is evident that when a larger amount of CFA was used, the structure remained intact. In contrast, when a smaller amount of CFA was used, the polymer melted. Additionally, the surface of the composite film was severely damaged, indicating that samples with added filler have a higher thermal resistance. The results have shown that the addition of CFA into LDPE enhanced the flammability of the composite by breaking the combustion cycle. Dhawan et al. [75] studied the flammability of RLDPE-CFA/TPP composite tiles. The results showed that the addition of TPP material decreased the flammability of the composite tile, characterized by a linear burning rate of 4.36 mm/min. The combustion of the composite tile was reduced due to the addition of CFA particles, as indicated by the decrease in its linear burning rate. The findings revealed that the incorporation of CFA engenders hindrance, leading to a retarded combustion rate and increased fire retardancy in the composite tiles. In this study, investigations were conducted on the morphological and structural characteristics, as well as the durability against various acids and bases, organic solvents, water absorption, and mechanical strength of composite tiles. The results obtained from the flammability test showed that the inclusion of TPP and CFA particles improved the fire-retardant properties of the composite tiles.

4.CONCLUSIONS

This review outlines the physical, morphological, and rheological properties of

polymer matrix composites reinforced with fly ash particles. The addition of fly ash into a polymer matrix significantly alters the overall properties of the resulting composites. Morphology analysis has revealed that proper processing methods and their parameters can result in uniformly distributed fly ash particles within a polymer matrix. Even in the presence of these findings, some particles were agglomerated and clustered; hence, the properties of the composite were affected. The application of fly ash improved the physical properties of the material, including density, water absorption, and thermal stability. The presence of fly ash influenced the rheological properties of the material, including its ability to store energy and the viscosity of the molten material. These effects vary in magnitude with the size, shape, and concentration of particles. This issue clearly articulates the detailed understanding gained from this analysis, which reveals that FA-filled low- and high-density polyethylene composites have great potential for use in a wide range of applications. Improved mechanical properties, better thermal stability, and recyclability make these composites highly useful in various application fields, including automotive, construction, and packaging. Processing parameters in future studies should be fine-tuned to achieve better dispersion of fly ash particles to reduce their tendency to agglomeration and enable the production of stronger and more durable composites. Furthermore, under long-term service conditions and variable environmental conditions, there is a need to study the performance of PE-FA composites to confirm whether they can be applicable and reliable in real-world applications. Moreover, another type of fly ash from different coal sources or even industrial production might create composites with variable characteristics for certain applications. Waste materials can be utilized to promote the development of fly-ash-filled LDPE and HDPE composites, aiming to ensure long-term sustainability in plastics.

REFERENCES

[1] Singh S, Ghorai MK, Kar KK. **Fly Ash-Reinforced Polyethylene Composites.** In: *Handbook of Fly Ash*. Elsevier; 2022:227-241.

[2] Hamada ML, Alwan GS, Annaz AA, Irhayyim SS, Hammood HS. **Experimental Investigation of Mechanical and Tribological Characteristics of Al 2024 Matrix Composite Reinforced by Yttrium Oxide Particles.** *Korean Journal of Materials Research* 2021; **31**(6):339-344.

[3] Krauklis AE, Karl CW, Gagani AI, Jørgensen JK. **Composite Material Recycling Technology—State-of-the-Art and Sustainable Development for the 2020s.** *Journal of Composites Science* 2021; **5**(1):28.

[4] Mahdi AD, Irhayyim SS, Abduljabbar SF. **Mechanical and Wear Behavior of Al7075 - Graphite Self-Lubricating Composite Reinforced by Nano-WO3 Particles.** *Materials Science Forum* 2020; **1002**:151-161.

[5] Barbero EJ. **Introduction to Composite Materials Design.** 3rd ed. 2017.

[6] Zaichenko N, Nefedov V. **Composite Material Based on the Polyethylene Terephthalate Polymer and Modified Fly Ash Filler.** *MATEC Web of Conferences* 2018; **245**:03007.

[7] Irhayyim SS, Hammood HS, Abdulhadi HA. **Effect of Nano-TiO2 Particles on Mechanical Performance of Al-CNT Matrix Composite.** *AIMS Materials Science* 2019; **6**(6):1124-1137.

[8] Zhang M, Biesold GM, Choi W, Yu J, Deng Y, Silvestre C. **Recent Advances in Polymers and Polymer Composites for Food Packaging.** *Materials Today* 2022; **53**:134-161.

[9] Nurazzi NM, Sabaruddin FA, Harussani MM, Kamarudin SH, Rayung M, Asyraf MRM. **Mechanical Performance and Applications of CNTs Reinforced Polymer Composites—A Review.** *Nanomaterials* 2021; **11**(9):2186.

[10] Atikler U, Basalp D, Tihminlioğlu F. **Mechanical and Morphological Properties of Recycled High-Density Polyethylene, Filled with Calcium Carbonate and Fly Ash.** *Journal of Applied Polymer Science* 2006; **102**(5):4460-4467.

[11] Mahesh V, Joladarashi S, Kulkarni SM. **A Comprehensive Review on Material Selection for Polymer Matrix Composites Subjected to Impact Load.** *Defence Technology* 2021; **17**(1): 257-277.

[12] Chohan JS, Boparai KS, Singh R, Hashmi MSJ. **Manufacturing Techniques and Applications of Polymer Matrix Composites: A Brief Review.** *Advances in Materials and Processing Technology* 2022; **8**(1):1103-1128.

[13] Bharath Kumar BR, Doddamani M, Zeltmann SE, Gupta N, Ramesh MR, Ramakrishna S. **Processing of Cenosphere/HDPE Syntactic Foams Using an Industrial Scale Polymer Injection Molding Machine.** *Materials and Design* 2016; **92**:414-423.

[14] Xavier FX. **Thermoplastic Polymer Composites: Processing, Properties, Performance, Applications and Recyclability.** John Wiley & Sons; 2022.

[15] Chawla KK. **Composite Materials: Science and Engineering.** 3rd ed. 2012.

[16] Cazan C, Cosnita M, Isac L. **The Influence of Temperature on the Performance of Rubber - PET-HDPE Waste -Based Composites with Different Inorganic Fillers.** *Journal of Cleaner Production* 2019; **208**:1030-1040.

[17] Chinh NT, Trang NTT, Mai TT, Giang NV, Trung TH, Huynh MD. **Thermal Properties, Thermo-Oxidation and UV-Thermo-Humidity Complex Stability of Polyethylene/Modified Fly Ash/Ultraflow Composites.** *Vietnam Journal of Chemistry* 2017; **55**(6):709-714.

[18] Ju S, Yoon J, Sung D, Pyo S. **Mechanical Properties of Coal Ash Particle-Reinferred Recycled Plastic-Based Composites for Sustainable Railway Sleepers.** *Polymers* 2020; **12**(10):2287.

[19] Acharjee SA, Bharali P, Gogoi B, Sorhie V, Walling B, Alemtoshi. **PHA-Based Bioplastic: A Potential Alternative to Address Microplastic Pollution.** *Water, Air, and Soil Pollution* 2023; **234**(1):21.

[20] Kazemi M, Faisal Kabir SF, Fini EH. **State of the Art in Recycling Waste Thermoplastics and Thermosets and Their Applications in Construction.** *Resources, Conservation and Recycling* 2021; **174**:105776.

[21] Jagadeesh P, Mavinkere Rangappa S, Siengchin S, Puttegowda M, Thiagamani SMK, Rajeshkumar G. **Sustainable Recycling Technologies for Thermoplastic Polymers and Their Composites: A Review of the State of the Art.** *Polymer Composites* 2022; **43**(9):5831-5866.

[22] Oladimeji Azeez T. **Thermoplastic Recycling: Properties, Modifications, and Applications.** In: *Thermosoftening Plastics*. 2020.

[23] Duta A, Cazan C, Cosnita M. **Fly Ash in Optimized Composites Based on Recycled Plastics and Rubber.** In: *World of Coal Ash (WOCA) Conference*. 2011:9-12.

[24] Anandhan S. **Recent Trends in Fly Ash Utilization in Polymer Composites.** *International Journal of Waste Resources* 2014; **4**(3):145.

[25] Oboh JO, Maliki D, Ajekwene KK, Salako O. **Effect of Hybrid Fillers of Bamboo Fiber and Commercial Glass Fiber on High Density Polyethylene Matrix.** *Journal of Applied Sciences and Environmental Management* 2022; **26**(5):897-903.

[26] Debnath K, Singh I. **Primary and Secondary Manufacturing of Polymer Matrix Composites.** 2017.

[27] Durowaye SI, Lawal GI, Sekunowo OI, Okonkwo EG. **Synthesis and Characterisation of Hybrid Polyethylene Terephthalate Matrix Composites Reinforced with Entada Mannii Fibre Particles and Almond Shell Particles.** *Journal of King Saud University - Engineering Sciences* 2019; **31**(4):322-327.

[28] Satapathy S, Kothapalli RVS. **Influence of Fly Ash Cenospheres on Performance of Coir Fiber-Reinforced Recycled High-Density Polyethylene Biocomposites.** *Journal of Applied Polymer Science* 2015; **132**(28):42222.

[29] Satapathy S, Nag A, Nando GB. **Thermoplastic Elastomers from Waste Polyethylene and Reclaim Rubber Blends and Their Composites with Fly Ash.** *Process Safety and Environmental Protection* 2010; **88**(2):131-141.

[30] Cosnita M, Balas M, Cazan C. **The Influence of Fly Ash on the Mechanical Properties of Water Immersed All Waste Composites.** *Polymers* 2022; **14**(10):1957.

[31] Mohd Nasir NH, Usman F, Saggaf A, Saloma. **Development of Composite Material from Recycled Polyethylene Terephthalate and Fly Ash: Four Decades Progress Review.** *Current Research in Green and Sustainable Chemistry* 2022; **5**:100280.

[32] Mohd Nasir NH, Usman F, Woen EL, Ansari MNM, Supian ABM. **Microstructural and Thermal Behaviour of Composite Material from Recycled Polyethylene Terephthalate and Fly Ash.** *Recycling* 2023; **8**(1):11.

[33] Mallick PK. **Processing of Polymer Matrix Composites.** 2017.

[34] Akay M. **An Introduction to Polymer Matrix Composites.** Irlandia: Ventus Publishing APs; 2015.

[35] Chinh NT, Mai TT, Trang NTT, Giang NV, Trung TH, Huong NTT. **Tensile, Electrical Properties and Morphology of Polyethylene/Modified Fly Ash Composites Using Ultraflow.** *Vietnam Journal of Chemistry* 2016; **54**(6):776-780.

[36] Sheykh MJ, Tarmian A, Doosthoseini K, Abdulkhani A. **Wear Resistance and Friction Coefficient of Nano-SiO2 and Ash-Filled HDPE/Lignocellulosic Fiber**

Composites. *Polymer Bulletin* 2017; **74**(11):4537-4547.

[37] Rotliwala YC, Parikh PA. **Thermal Co-processing of High Density Polyethylene with Coal, Fly Ashes, and Biomass: Characterization of Liquid Products.** *Energy Sources, Part A: Recovery, Utilization, and Environmental Effects* 2012; **34**(11): 1055-1066.

[38] Satapathy S, Nando GB, Nag A, Raju KVSN. **HDPE-Fly Ash/Nano Fly Ash Composites.** *Journal of Applied Polymer Science* 2013; **130**(6):3998-4007.

[39] Porcino DD, Mauriello F, Bonaccorsi L, Tomasello G, Paone E, Malara A. **Recovery of Biomass Fly Ash and HDPE in Innovative Synthetic Lightweight Aggregates for Sustainable Geotechnical Applications.** *Sustainability* 2020; **12**(16):6552.

[40] Baglari S, Kole M, Dey TK. **Effective Thermal Conductivity and Coefficient of Linear Thermal Expansion of High-Density Polyethylene — Fly Ash Composites.** *Indian Journal of Physics* 2011; **85**(4):559-573.

[41] Satapathy S, Kothapalli RVS. **Mechanical, Dynamic Mechanical and Thermal Properties of Banana Fiber/Recycled High Density Polyethylene Biocomposites Filled with Flyash Cenospheres.** *Journal of Polymers and the Environment* 2018; **26**(1):200-213.

[42] Verma P, Kumar A, Chauhan SS, Verma M, Malik RS, Choudhary V. **Industrially Viable Technique for the Preparation of HDPE/Fly Ash Composites at High Loading: Thermal, Mechanical, and Rheological Interpretations.** *Journal of Applied Polymer Science* 2018; **135**(11):45995.

[43] Sear A. **Properties and Use of Coal Fly Ash: A Valuable Industrial By-Product.** 2001.

[44] Salah N, Alfawzan AM, Saeed A, Alshahrie A, Allafi W. **Effective Reinforcements for Thermoplastics Based on Carbon Nanotubes of Oil Fly Ash.** *Scientific Reports* 2019; **9**(1):20288.

[45] Kaleni A, Magagula SI, Motloung MT, Mochane MJ, Mokhena TC. **Preparation and Characterization of Coal Fly Ash Reinforced Polymer Composites: An Overview.** *Express Polymer Letters* 2022; **16**(7):693-726.

[46] Yao J, Li W, Xia F, Zheng Y, Fang C, Shen D. **Heavy Metals and PCDD/Fs in Solid Waste Incinerator Fly Ash in Zhejiang Province, China: Chemical and Bio-Analytical Characterization.** *Environmental Monitoring and Assessment* 2012; **184**(6):3711-3720.

[47] Wang X, Fu C, Feng Z, Huo H, Yin X, Gao G. **Flyash/Polymer Composite Electrolyte with Internal Binding Interaction Enables Highly-Stable Extrinsic-Interfaces of All-Solid-State Lithium Batteries.** *Chemical Engineering Journal* 2022; **428**:131041.

[48] Khan MJ, Al-Juhani AA, Shawabkeh R, Ul-Hamid A, Hussein IA. **Chemical Modification of Waste Oil Fly Ash for Improved Mechanical and Thermal Properties of Low Density Polyethylene Composites.** *Journal of Polymer Research* 2011; **18**(6):2275-2284.

[49] Senapati AK, Bhatta A, Mohanty S, Mishra PC, Routra BC. **An Extensive Literature Review on the Usage of Fly Ash as a Reinforcing Agent for Different Matrices.** *International Journal of Innovative Science and Modern Engineering* 2014; **3**(1):1-5.

[50] Tambrallimath V, Keshavamurthy R, Davim P, Pradeep Kumar GS, Pignatta G, Badari A. **Synthesis and Characterization of Flyash Reinforced Polymer Composites Developed by Fused Filament Fabrication.** *Journal of Materials Research and Technology* 2022; **21**: 2420-2433.

[51] Dadkar N, Tomar BS, Satapathy BK. **Evaluation of Flyash-Filled and Aramid Fibre Reinforced Hybrid Polymer Matrix Composites (PMC) for Friction Braking Applications.** *Materials and Design* 2009; **30**(10): 4369-4375.

[52] Kasar AK, Gupta N, Rohatgi PK, Menezes PL. **A Brief Review of Fly Ash as Reinforcement for Composites with Improved Mechanical and Tribological Properties.** *JOM* 2020; **72**(6):2340-2351.

[53] Tang Z, Deng N. **Effect of Salt Solution on the Mechanical Behaviours of Geopolymer Concrete under Dry-Wet Cycles.** *Advances in Materials Science and Engineering* 2022; **2022**:1-9.

[54] Deepthi MV, Sharma M, Sailaja RRN, Anantha P, Sampathkumaran P, Seetharamu S. **Mechanical and Thermal Characteristics of High Density Polyethylene–Fly Ash Cenospheres Composites.** *Materials and Design* 2010; **31**(4):2051-2060.

[55] Chand N, Sharma P, Fahim M. **Abrasive Wear Behavior of LDPE Filled with Silane Treated Flyash Cenospheres.** *Composite Interfaces* 2011; **18**(7):575-586.

[56] Chand N, Sharma P, Fahim M. **Correlation of Mechanical and Tribological Properties of Organosilane Modified Cenosphere Filled High Density Polyethylene.** *Materials Science and Engineering: A* 2010; **527**(21-22):5873-5878.

[57] Minchenkov K, Vedernikov A, Safonov A, Akhatov I. **Thermoplastic Pultrusion: A Review.** *Polymers* 2021; **13**(2):180.

[58] Esfandiari P, Silva JF, Novo PJ, Nunes JP, Marques AT. **Production and Processing of Pre-Impregnated Thermoplastic Tapes by Pultrusion and Compression Moulding.** *Journal of Composite Materials* 2022; **56**(11):1731-1746.

[59] Kar KK. **Composite Materials.** Springer Berlin Heidelberg: Berlin, Heidelberg; 2017.

[60] Alshammari BA, Alsuhybani MS, Almushaikeh AM, Alotaibi BM, Alenad AM, Alqahtani NB. **Comprehensive Review of the Properties and Modifications of Carbon Fiber-Reinforced Thermoplastic Composites.** *Polymers* 2021; **13**(15):2474.

[61] Ahmad I, Mahanwar PA. **Mechanical Properties of Fly Ash Filled High Density Polyethylene.** *Journal of Minerals and Materials Characterization and Engineering* 2010; **9**(3):183-188.

[62] Satapathy S, Nag A, Nando GB. **Effect of Electron Beam Irradiation on the Mechanical, Thermal, and Dynamic Mechanical Properties of Flyash and Nanostructured Fly Ash Waste Polyethylene Hybrid Composites.** *Polymer Composites* 2012; **33**(1):109-119.

[63] Satapathy S, Bihari Nando G. **Mechanical, Dynamic Mechanical, and Thermal Characterization of Fly Ash and Nanostructured Fly Ash-Waste Polyethylene/High-Density Polyethylene Blend Composites.** *Polymer Composites* 2016; **37**(11):3256-3268.

[64] Divya VC, Khan MA, Rao BN, Sailaja RRN, Vynatheya S, Seetharamu S. **Fire Retardancy Characteristics and Mechanical Properties of High-Density Polyethylene/Ultrafine Fly Ash/MWCNT Nanocomposites.** *Polymer-Plastics Technology and Engineering* 2017; **56**(7):762-776.

[65] Kabir II, Sorrell CC, Mada MR, Cholake ST, Bandyopadhyay S. **General Model for Comparative Tensile Mechanical Properties of Composites Fabricated from Fly Ash and Virgin/Recycled High-Density Polyethylene.** *Polymer Engineering and Science* 2016; **56**(10):1096-1108.

[66] Satapathy S. **Development of Value-Added Composites from Recycled High-Density Polyethylene, Jute Fiber and Flyash Cenospheres: Mechanical, Dynamic Mechanical and Thermal Properties.** *International Journal of Plastics Technology* 2018; **22**(2):386-405.

[67] Patil B, Bharath Kumar BR, Doddamani M. **Compressive Behavior of Fly Ash Based 3D Printed Syntactic Foam Composite.** *Materials Letters* 2019; **254**:246-249.

[68] Alghamdi MN. **Effect of Filler Particle Size on the Recyclability of Fly Ash Filled HDPE Composites.** *Polymers* 2021; **13**(16):2836.

[69] Wu A, Jia L, Yu W, Zhu F, Liu F, Wang Y. **Preparation and Finite Element Analysis of Fly Ash/HDPE Composites for Large Diameter Bellows.** *Polymers* 2021; **13**(23):4204.

[70] Alghamdi MN. **Performance for Fly Ash Reinforced HDPE Composites over the Ageing of Material Components.** *Polymers* 2022; **14**(14):2913.

[71] Omair N, Intan Syaqirah MZ. **Mechanical Properties of Recycled High-Density Polyethylene, Rice Husk Ash, and Fly Ash Composite Mixture.** *Journal of Innovation and Technology* 2022; **2022**(22):1-8.

[72] Khan MJ, Al-Juhani AA, Ul-Hamid A, Shawabkeh R, Hussein IA. **Effect of Chemical Modification of Oil Fly Ash and Compatibilization on the Rheological and Morphological Properties of Low-Density Polyethylene Composites.** *Journal of Applied Polymer Science* 2011; **122**(4):2486-2496.

[73] Adeosun SO, Usman MA, Akpan EI, Dibie WI. **Characterization of LDPE Reinforced with Calcium Carbonate—Fly Ash Hybrid Filler.** *Journal of Minerals and Materials Characterization and Engineering* 2014; **2**(4):334-345.

[74] Porabka A, Jurkowski K, Laska J. **Fly Ash Used as a Reinforcing and Flame-Retardant Filler in Low-Density Polyethylene.** *Polimery* 2015; **60**(4):251-257.

[75] Dhawan R, Bisht BMS, Kumar R, Kumari S, Dhawan SK. **Recycling of Plastic Waste into Tiles with Reduced**

Flammability and Improved Tensile Strength. *Process Safety and Environmental Protection* 2019; **124**:299-307.

[76] Sim J, Kang Y, Kim BJ, Park YH, Lee YC. **Preparation of Fly Ash/Epoxy Composites and Its Effects on Mechanical Properties.** *Polymers* 2020; **12**(1):79.

[77] Chen P, Wang Y, Li J, Chu W. **Synergetic Effect of Fly Ash Cenospheres and Multi-Walled Carbon Nanotubes on Mechanical and Tribological Properties of Epoxy Resin Coatings.** *Journal of Applied Polymer Science* 2021; **138**(32):50789.

[78] Jinnai H, Spontak RJ. **Transmission Electron Microtomography in Polymer Research.** *Polymer* 2009; **50**(5):1067-1087.

[79] Kumar CSSR. **Transmission Electron Microscopy Characterization of Nanomaterials.** Springer Berlin Heidelberg: Berlin, Heidelberg; 2014.

[80] Dasari A, Yu Z-Z, Mai Y-W. **Polymer Nanocomposites.** Springer London: London; 2016.

[81] Chen H, Ginzburg VV, Yang J, Yang Y, Liu W, Huang Y. **Thermal Conductivity of Polymer-Based Composites: Fundamentals and Applications.** *Progress in Polymer Science* 2016; **59**:41-85.

[82] Agari Y, Uno T. **Estimation on Thermal Conductivities of Filled Polymers.** *Journal of Applied Polymer Science* 1986; **32**(7):5705-5712.

[83] Huang R, Xu X, Lee S, Zhang Y, Kim B-J, Wu Q. **High Density Polyethylene Composites Reinforced with Hybrid Inorganic Fillers: Morphology, Mechanical and Thermal Expansion Performance.** *Materials* 2013; **6**(9): 4122-4138.

[84] Elfaleh I, Abbassi F, Habibi M, Ahmad F, Guedri M, Nasri M. **A Comprehensive Review of Natural Fibers and Their Composites: An Eco-Friendly Alternative to Conventional Materials.** *Results in Engineering* 2023; **19**:101271.

[85] Yu S, Lee J, Kim J, Chang H, Kang C, Sim J. **Analysis of Mechanical Properties and Structural Analysis According to the Multi-Layered Structure of Polyethylene-Based Self-Reinforced Composites.** *Polymers* 2023; **15**(20):4055.

[86] Mishra P. **Mechanical Behavior of Bagasse Fiber Reinforced Epoxy Composites at Liquid Nitrogen Temperature.** *Journal of Solid Waste Technology and Management* 2014; **40**(3):197-202.

[87] Mazur K, Jakubowska P, Romańska P, Kuciel S. **Green High Density Polyethylene (HDPE) Reinforced with Basalt Fiber and Agricultural Fillers for Technical Applications.** *Composites Part B: Engineering* 2020; **202**:108399.

[88] Ahmad S, Dawood O, Lashin MMA, Khattak SU, Javed MF, Aslam F. **Effect of Coconut Fiber on Low-Density Polyethylene Plastic-Sand Paver Blocks.** *Ain Shams Engineering Journal* 2023; **14**(8):101982.

[89] Bazgir H, Sepahi A, Hosseini S, Afzali K, Houshmandmoayed S, Nikzinat E. **Clarifying Effect of Multimodal Polymerization on Thermal, Rheological, and Mechanical Properties of HDPE Pipe Resin.** *Journal of Polymer Research* 2023; **30**(2):58.

[90] Zeraatpishe M, Hassanajili S. **Investigation of Physical and Rheological Properties of LDPE/HDPE/Thermoplastic Starch Biodegradable Blend Films.** *Polymer Engineering and Science* 2023; **63**(9):3116-3134.

[91] Gong Y, Wang S-H, Zhang Z-Y, Yang X-L, Yang Z-G, Yang H-G. **Degradation of Sunlight Exposure on the High-Density Polyethylene (HDPE) Pipes for Transportation of Natural Gases.** *Polymer Degradation and Stability* 2021; **194**:109752.

[92] Pattanaik A, Mukharjee M, Mishra SC. **Effect of Environmental Aging Conditions on the Properties of Fly Ash Filled Epoxy Composites.** *Advanced Composite Materials* 2020; **29**(1):1-30.

[93] Starkova O, Gagani AI, Karl CW, Rocha IBCM, Burlakovs J, Krauklis AE. **Modelling of Environmental Ageing of Polymers and Polymer Composites—Durability Prediction Methods.** *Polymers* 2022; **14**(5):907.

[94] Rocha JS, Escócio VA, Visconte LL, Pacheco ÉB. **Thermal and Flammability Properties of Polyethylene Composites with Fibers to Replace Natural Wood.** *Journal of Reinforced Plastics and Composites* 2021; **40**(19-20):726-740.

[95] Zhang J, Koubaa A, Xing D, Wang H, Wang F, Wang X-M, Wang Q. **Flammability, Thermal Stability, and Mechanical Properties of Wood Flour/Polycarbonate/Polyethylene Bio-Based Composites.** *Industrial Crops and Products* 2021; **169**:113638.